# Appendix C: Air Quality Modeling

## Introduction

This appendix describes in greater detail the various methodologies used to translate differences in control and no-control scenario emission estimates into changes in air quality conditions. Summary characterizations of the results of the air quality modeling efforts for 1990 are provided here and in the main text. Further details and discussion of key analytical and modeling issues can be found in a number of supporting documents. These documents, which provide the analytical basis for the results presented herein, are:

- ICF Kaiser/Systems Applications International, *"Retrospective Analysis of Ozone Air Quality in the United States"*, Final Report, May 1995. (Hereafter referred to as "SAI Ozone Report (1995).")

- ICF Kaiser/Systems Applications International, "*Retrospective Analysis of Particulate Matter Air Quality in the United States"*, Draft Report, September 1992. (Hereafter referred to as "SAI PM Report (1992).")

- ICF Kaiser/Systems Applications International, "*Retrospective Analysis of Particulate Matter Air Quality in the United States"*, Final Report, April 1995. (Hereafter referred to as "SAI PM Report (1995).")

- ICF Kaiser/Systems Applications International, *"PM Interpolation Methodology for the section 812 retrospective analysis"*, Memorandum from J. Langstaff to J. DeMocker, March 1996. (Hereafter referred to as "SAI PM Interpolation Memo (1996).")

- ICF Kaiser/Systems Applications International, *"Retrospective Analysis of $SO_2$, $NO_x$ and CO Air Quality in the United States"*, Final Report, November 1994. (Hereafter referred to as "SAI $SO_2$, $NO_x$ and CO Report (1994).")

- ICF Kaiser/Systems Applications International, "*Retrospective Analysis of the Impact of the Clean Air Act on Urban Visibility in the Southwestern United States"*, Final Report, October 1994. (Hereafter referred to as "SAI SW Visibility Report (1994).")

- Dennis, Robin L., US EPA, ORD/NERL, *"Estimation of Regional Air Quality and Deposition Changes Under Alternative 812 Emissions Scenarios Predicted by the Regional Acid Deposition Model, RADM"*, Draft Report, October 1995. (Hereafter referred to as "RADM Report (1995).")

The remainder of this appendix describes, for each pollutant or air quality effect of concern, (a) the basis for development of the control scenario air quality profiles; (b) the air quality modeling approach used to estimate differences in air quality outcomes for the control and no-control scenario and the application of those results to the derivation of the no-control scenario air quality profiles; (c) the key assumptions, caveats, analytical issues, and limitations associated with the modeling approach used; and (d) a summary characterization of the differences in estimated air quality outcomes for the control and no-control scenarios.

## Carbon Monoxide

### Control scenario carbon monoxide profiles

As described in the preceding general methodology section, the starting point for development of control scenario air quality profiles was EPA's AIRS da-

Table C-1. Summary of CO Monitoring Data.

| Year | Number of Monitors | Number of Counties | Percent Population Covered | Number of Samples | Mean Number of Samples per Monitor |
|---|---|---|---|---|---|
| **1970** | 82 | 54 | n/a | 408,524 | 4,982 |
| **1975** | 503 | 246 | n/a | 2,667,525 | 5,303 |
| **1980** | 522 | 250 | 50 % | 3,051,599 | 5,846 |
| **1985** | 472 | 232 | n/a | 3,533,286 | 7,486 |
| **1990** | 506 | 244 | 55 % | 3,788,053 | 7,486 |

Data Source: SAI $SO_2$, $NO_x$ and CO Report (1994).

tabase. Hourly CO air quality monitoring data were compiled for all monitors in the 48 contiguous states for the study target years of 1970, 1975, 1980, 1985, and 1990. Although the CO monitoring network was sparse in 1970, by 1990 506 monitors in 244 counties provided monitoring coverage for 55 percent of the population in the conterminous U.S. Table C-1 summarizes the CO monitoring data derived from AIRS. Additional data regarding the EPA Region location, land use category, location-setting category, and objective category of the monitors providing these data are described in the SAI $SO_2$, $NO_x$, and CO Report (1994).

The next step in constructing the control scenario air quality profiles was to calculate moving averages, for a variety of time periods, of the hourly CO data for each monitor. For CO, moving averages of 1, 3, 5, 7, 8, 12, and 24 hours were calculated. Daily maximum concentrations observed at each monitor for each of these averaging periods were then calculated. Finally, profiles were developed to reflect the average and maximum concentrations for each of the seven averaging periods. However, profiles were only developed for a given monitor when at least 10 percent of its theoretically available samples were actually available. The purpose of applying this cutoff was to avoid inclusion of monitors for which available sample sizes were too small to provide a reliable indication of historical air quality.

As discussed in the air quality modeling chapter of the main text, development of representative distributions for these profiles was then necessary to provide a manageable characterization of air quality conditions. Initially, two-parameter lognormal distributions were fitted to the profiles based on substantial evidence that such distributions are appropriate for modeling air quality data. However, given the relative importance of accurately modeling higher percentile observations (i.e., 90th percentile and higher), a three-parameter modeling approach was used to isolate the effect of observations equal, or very close, to zero. In this approach one parameter defines the proportion of data below a cutoff close to zero and the remaining two parameters describe the distribution of data above the cutoff value. Several other studies have already demonstrated good fit to air quality modeling data with a three-parameter gamma distribution, and both lognormal and gamma distributions using a three-parameter approach were developed for the present study. As documented in the SAI $SO_2$, $NO_x$, and CO Report (1994), a cutoff of 0.05 ppm was applied and both the three-parameter lognormal and three-parameter gamma distributions provided a good fit to the empirical data. For CO, the gamma distribution provided the best fit.

The control scenario air quality profiles are available on diskette. The filename for the CO Control Scenario profile database is COCAA.DAT, and adopts the format presented in Table C-2.

### *No-control scenario carbon monoxide profiles*

To derive comparably configured profiles representing CO air quality in the no-control scenario, control scenario profile means and variances were adjusted in proportion to the difference in emissions estimated under the two scenarios. Specifically, for all control scenario air quality observations predicted by the three-parameter distributions falling above the "near-zero" cutoff level, comparable no-control estimates were derived by the following equation:

Table C-2. Format of Air Quality Profile Databases.

| Columns | Format | Description |
|---|---|---|
| 1 - 2 | Integer | Year (70, 75, 80, 85, 90) |
| 4 - 6 | Integer | Averaging time (1, 3, 5, 7, 8, 12, 24 hours) |
| 8 - 9 | Integer | State FIPS code |
| 11 - 13 | Integer | County FIPS code |
| 15 - 19 | Integer | Monitor number (digits 6-10 of monitor id) |
| 21 - 30 | Real | Latitude |
| 32 - 41 | Real | Longitude |
| 43 - 44 | Integer | Latitude/longitude flag[a] |
| 46 - 55 | Real (F10.3) | Hourly intermittency parameter $p$[b] |
| 56 - 65 | Real (F10.3) | Hourly lognormal parameter $\mu$[b] |
| 66 - 75 | Real (F10.3) | Hourly lognormal parameter $\sigma$[b] |
| 76 - 85 | Real (F10.3) | Hourly gamma parameter $\alpha$[b] |
| 86 - 95 | Real (F10.3) | Hourly gamma parameter $\beta$[b] |
| 96 - 105 | Real (F10.3) | Daily max intermittency parameter $p$[b] |
| 106 - 115 | Real (F10.3) | Daily max lognormal parameter $\mu$[b] |
| 116 - 125 | Real (F10.3) | Daily max lognormal parameter $\sigma$[b] |
| 126 - 135 | Real (F10.3) | Daily max gamma parameter $\alpha$[b] |
| 136 - 145 | Real (F10.3) | Daily max gamma parameter $\beta$[b] |

[a] Values for flag: 1 = actual latitude/longitude values
2 = latitude/longitude values from collocated monitor or previous monitor location (monitor parameter occurrence code 1)
-9 = latitude/longitude missing (county center substituted)

[b] Units of concentration are ppm for CO and ppb for $SO_2$, $NO_2$ and NO.

Source: SAI $SO_2$, $NO_x$ and CO Report (1994).

$$X_{NC} = \left(\frac{E_{NC}}{E_C}\right)(X_C - b) + b \qquad (1)$$

where

$X_{NC}$ = air quality measurement for the no-control scenario,
$X_C$ = air quality measurement for the control scenario,
$E_{NC}$ = emissions estimated for the no-control scenario,
$E_C$ = emissions estimated for the control scenario, and
$b$ = background concentration.

The adjustment for background concentration is made to hold ambient background concentrations of the pollutant constant between the control and no-control scenarios. To the extent background concentrations are affected by transport of anthropogenic pollutants from upwind sites, and to the extent upwind emissions may have been controlled under the control scenario, assuming a fixed background concentration represents a conservative assumption in this analysis. As discussed in the SAI $SO_2$, $NO_x$, and CO Report (1994), the CO background concentration used for this analysis was 0.2 ppm, which equals the lowest typical concentration observed in the lower 48 states.

In the SAI $SO_2$, $NO_x$, and CO Report (1994) documenting the CO air quality modeling effort, reference is made to using county-level emission estimates as the basis for deriving the no-control profiles. Derivation of these county-level results is described in more detail in the appendix on emissions estimation. It is important to emphasize here, however, that the county-level CO emissions data were derived for both the control and no-control scenarios by simple population-weighted disaggregation of state-level emission totals. Although CO emission estimates were needed at the county level to support the ozone air quality modeling effort, differences in state-level emissions estimates are what drive the difference in the control and no-control air quality profiles for CO. In other words, the $E_{NCAA}$ to $E_{CAA}$ ratios used to derive the no-control profiles according to Equation (1) above are essentially based on state-level emissions estimates for CO.

As for the control scenario air quality profiles, the no-control scenario air quality profiles are available on diskette. The filename for the CO No-control Scenario profile database is CONCAA.DAT. The same data format described in Table C-2 is adopted.

### Summary differences in carbon monoxide air quality

While the control and no-control scenario air quality profiles are too extensive to present in their entirety in this report, a summary indication of the difference in control and no-control scenario CO concentrations is useful. Figure C-1 provides this summary characterization. Specifically, the air quality indicator provided is the 95th percentile observation of 1990 CO concentrations averaged over a 1-hour period. The graph shows the number of monitors for which the ratio of 1990 control to no-control scenario 95th percentile 1-hour average concentrations falls within a particular range. The x-axis values in the graph represent the midpoint of each bin. The results indicate that, by 1990, CO concentrations under a no-control scenario would have been dramatically higher than control scenario concentrations.

Figure C-1. Frequency Distribution of Estimated Ratios for 1990 Control to No-control Scenario 95th Percentile 1-Hour Average CO Concentrations, by Monitor.

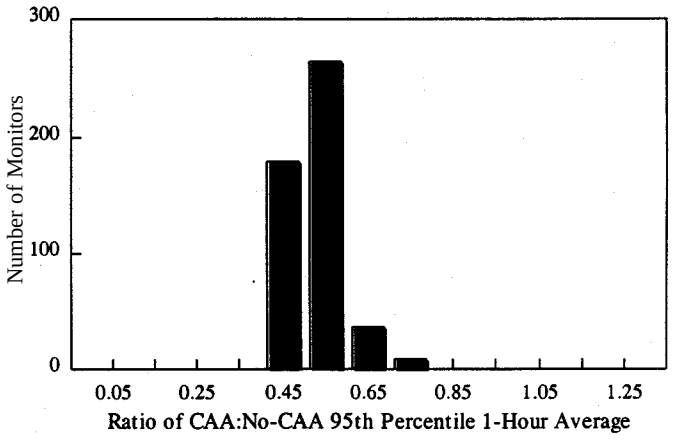


### Key caveats and uncertainties for carbon monoxide

A number of important uncertainties should be noted regarding the CO air quality estimates used in this analysis. First and foremost, CO is a highly localized, "hot spot" pollutant. As such, CO monitors are often located near heavily-used highways and intersections to capture the peak concentrations associated with mobile sources. Since this analysis relies on state-level aggregate changes in CO emissions from all sources, the representativeness and accuracy of the predicted CO air quality changes are uncertain. There is no basis, however, for assuming any systematic bias which would lead to over- or under-estimation of air quality conditions due to reliance on state-wide emission estimates.

A second source of uncertainty is the extent to which the three-parameter distributions adequately characterize air quality indicators of concern. Appendix C of the SAI $SO_2$, $NO_x$, and CO Report (1994) presents a number of graphs comparing the fitted versus empirical data for one-hour and 12-hour averaging periods. In the case of CO, the gamma distribution appears to provide a very reasonable fit, though clearly some uncertainty remains.

Finally, a central premise of this analysis is that changes in CO emissions should be well-correlated with changes in CO air quality. Strong correlation between the state-level emissions estimates used in this analysis and empirical air quality measurements would not be expected due to inconsistencies between the state-level scale of modeled emissions versus the monitor-level scale of the air quality data, and between the modeled control scenario emissions inventories and actual historical air quality measurements. Under these circumstances, it is particularly important to focus on the primary objective of the current analysis, which is to estimate the difference in air quality outcomes between scenarios which assume the absence or presence of historical air pollution controls. In the process of taking differences, some of the uncertainties are expected to cancel out. No attempt is made in the overall analysis to predict historical air quality, or hypothetical air quality in the absence of the Clean Air Act, in absolute terms.

Table C-3. Summary of $SO_2$ Monitoring Data.

| Year | Number of Monitors | Number of Counties | Percent Population Covered | Number of Samples | Mean Number of Samples per Monitor |
|---|---|---|---|---|---|
| **1970** | 86 | 56 | n/a | 399,717 | 4,648 |
| **1975** | 847 | 340 | n/a | 4,280,303 | 5,053 |
| **1980** | 1,113 | 440 | 60 % | 6,565,589 | 5,899 |
| **1985** | 926 | 401 | n/a | 6,602,615 | 7,130 |
| **1990** | 769 | 374 | 50 % | 5,810,230 | 7,556 |

Data Source: SAI $SO_2$, $NO_x$ and CO Report (1994).

## Sulfur Dioxide

Sulfur dioxide ($SO_2$) emissions lead to several air quality effects, including secondary formation of fine particle sulfates, long range transport and deposition of sulfuric acid, and localized concentrations of gaseous sulfur dioxide. The first two effects are addressed later in this appendix, under the particulate matter and acid deposition sections. The focus of this section is estimation of changes in local concentrations of sulfur dioxide.

The methodology applied to estimation of local sulfur dioxide air quality is essentially identical to the one applied for carbon monoxide. As such, this section does not repeat the "roll-up" modeling methodological description presented in the CO section, but instead simply highlights those elements of the sulfur dioxide modeling which differ from carbon monoxide.

### Control scenario sulfur dioxide profiles

Unlike the CO monitoring network, the number of monitors as well as the population coverage of the $SO_2$ monitoring network shrank during the 1980's. Table C-3 summarizes the $SO_2$ monitoring data used as the basis for development of the control scenario air quality profiles.

As for CO, air quality profiles reflecting average values and daily maxima for 1, 3, 5, 7, 8, 12, and 24 hour averages were compiled from AIRS for monitors in the lower 48 states which had at least 10 percent of their potential samples available. Applying a cutoff of 0.1 ppb to isolate the zero and near-zero observations, three-parameter lognormal and gamma distributions were fitted to these empirical profiles. In the case of $SO_2$, the three-parameter lognormal distribution was found to provide the best fit.

The control scenario $SO_2$ air quality profiles are available on diskette, contained in a file named SO2CAA.DAT. The same data format described in Table C-2 is adopted.

### No-control scenario sulfur dioxide profiles

The no-control air quality profiles for $SO_2$ are derived using Equation 1, the same equation used for CO. For $SO_2$, the background concentration was assumed to be zero. Although anthropogenic emissions contribute only small amounts to total global atmospheric sulfur, measured background concentrations

for the continental U.S. range from only 0.1 to 1.3 ppb. Background $SO_2$ is discussed in more detail in the supporting document SAI $SO_2$, $NO_x$, and CO Report (1994).[1]

The no-control scenario $SO_2$ air quality profiles are available on diskette, contained in a file named SO2NCAA.DAT. The data format is described in Table C-2.

### Summary differences in sulfur dioxide air quality

As for CO, reporting differences in control and no-control scenario air quality projections for each monitor covered in the analysis is impractical due to the large amount of data involved. However, Figure C-2 provides an illustration of scenario differences similar to the one provided for CO. Specifically, the graph shows the distribution of 1990 control to no-control scenario 95th percentile 1-hour average concentrations ratios at $SO_2$ monitors. By 1990, $SO_2$ concentrations under the no-control scenario were substantially higher than those associated with the control scenario.

Figure C-2. Frequency Distribution of Estimated Ratios for 1990 Control to No-control Scenario 95th Percentile 1-Hour Average $SO_2$ Concentrations, by Monitor.

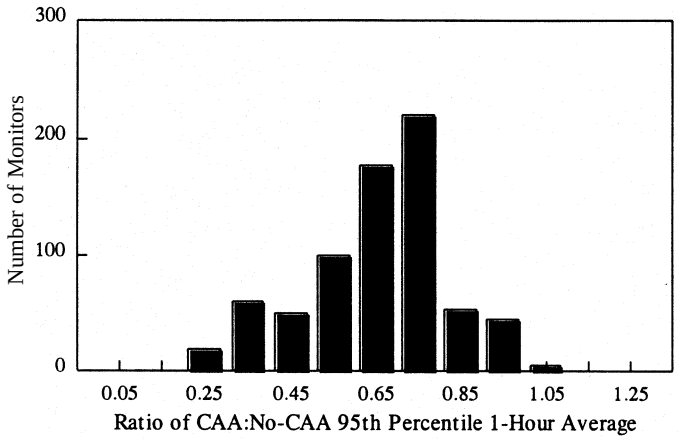


### Key caveats and uncertainties for sulfur dioxide

The height of stacks used to vent flue gases from utility and industrial fossil fuel-fired boilers has a significant effect on the dispersion of sulfur dioxide and on the formation and long-range transport of secondary products such as particulate sulfates. Under a no-control scenario, it is conceivable that some sources might have built taller stacks to allow higher emission rates without creating extremely high ground-level concentrations of flue gases. On the other hand, it is also conceivable that, in the absence of post-1970 air pollution control programs, sources might have built shorter stacks to avoid incurring the higher costs associated with building and maintaining taller stacks. To the extent facilities would have adopted different stack height configurations under a no-control scenario, both local exposures to sulfur dioxides (and other emissions from fossil fuel combustion) and long-range transport, deposition, and exposure associated with secondary formation products may have been different. However, this analysis assumes that both the location of individual facilities and the height and configuration of emission stacks are constant between the two scenarios. If, in fact, stack heights were raised under the historical case due to CAA-related concerns, increases in local $SO_2$ concentrations under the no-control scenario may be overestimated. However, this same assumption may at the same time lead to underestimation under the no-control scenario of long-range transport and formation of secondary particulates associated with taller stacks. For stacks built lower under a no-control scenario, local $SO_2$ exposures would have been higher and long-range effects lower. Finally, the comments on uncertainties for carbon monoxide apply as well to $SO_2$.

## Nitrogen Oxides

Similarly to sulfur dioxide, emissions of nitrogen oxides ($NO_x$) –including nitrogen dioxide ($NO_2$) and nitrous oxide (NO)– lead to several air quality effects. These effects include secondary formation of fine particle nitrates, formation of ground-level ozone, long range transport and deposition of nitric acid, and localized concentrations of both $NO_2$ and NO. The first three effects are addressed later in this appendix, under the particulate matter, ozone, and acid deposition sections. The focus of this section is estimation of changes in local concentrations of $NO_2$ and NO.

The methodology applied to estimation of local nitrogen oxides air quality is essentially identical to the one applied for carbon monoxide and sulfur dioxide. As such, this section does not repeat the "roll-up" modeling methodological description presented in the CO section, but instead simply highlights those ele-

[1] SAI $SO_2$, NOx, and CO Report (1994), page 4-9.

ments of the nitrogen oxides modeling which differ from carbon monoxide.

### *Control scenario nitrogen oxides profiles*

After peaking around 1980, the number of $NO_2$ and NO monitors, their county coverage, and their population coverage shrank between 1980 and 1990. Tables C-4 and C-5 summarize, respectively, the $NO_2$ and NO monitoring data used as the basis for development of the control scenario air quality profiles.

As for CO and $SO_2$, air quality profiles reflecting average values and maxima for 1, 3, 5, 7, 8, 12, and 24 hour $NO_2$ and NO averages were compiled from AIRS for monitors in the lower 48 states which had at least 10 percent of their potential samples available. Applying a cutoff of 0.5 ppb to both $NO_2$ and NO to isolate the zero and near-zero observations, three-parameter lognormal and gamma distributions were fitted to these empirical profiles. For $NO_2$ and NO, the three-parameter gamma distribution was found to provide the best fit.

The control scenario $NO_2$ and NO air quality profiles are available on diskette, contained in files named NO2CAA.DAT and NOCAA.DAT, respectively. The same data format described in Table C-2 is adopted.

Table C-4. Summary of $NO_2$ Monitoring Data.

| Year | Number of Monitors | Number of Counties | Percent Population Covered | Number of Samples | Mean Number of Samples per Monitor |
|---|---|---|---|---|---|
| **1970** | 45 | 32 | n/a | 275,534 | 6,123 |
| **1975** | 308 | 155 | n/a | 1,574,444 | 5,112 |
| **1980** | 379 | 205 | 45 % | 1,984,128 | 5,235 |
| **1985** | 305 | 182 | n/a | 2,142,606 | 7,025 |
| **1990** | 346 | 187 | 40 % | 2,456,922 | 7,101 |

Data Source: SAI $SO_2$, $NO_x$ and CO Report (1994).

Table C-5. Summary of NO Monitoring Data.

| Year | Number of Monitors | Number of Counties | Percent Population Covered | Number of Samples | Mean Number of Samples per Monitor |
|---|---|---|---|---|---|
| **1970** | 39 | 28 | n/a | 246,262 | 6,314 |
| **1975** | 206 | 94 | n/a | 1,101,051 | 5,345 |
| **1980** | 224 | 124 | 30 % | 1,023,834 | 4,571 |
| **1985** | 139 | 86 | n/a | 956,425 | 6,881 |
| **1990** | 145 | 81 | 15 % | 999,808 | 6,895 |

Data Source: SAI $SO_2$, $NO_x$ and CO Report (1994).

### No-control scenario nitrogen oxides profiles

The no-control air quality profiles for $NO_2$ and NO are derived using Equation 1, the same equation used for CO and $SO_2$. As discussed in detail in the SAI $SO_2$, $NO_x$, and CO Report (1994),[2] nitrogen oxides are emitted almost entirely from anthropogenic sources and they do not have long atmospheric residence times. Therefore, global background concentrations are very low, on the order of 0.1 or 0.2 ppb. For the present analysis, background concentrations of $NO_2$ and NO were assumed to be zero.

The no-control scenario $NO_2$ and NO air quality profiles are available on diskette, contained in files named NO2NCAA.DAT and NONCAA.DAT, respectively. The data format is described in Table C-2.

### Summary differences in nitrogen oxides air quality

Figure C-3 provides a summary indication of the differences in control and no-control scenario air quality for $NO_2$. As for CO and $SO_2$, the graph shows the distribution of 1990 control to no-control scenario 95th percentile 1–hour average concentration ratios at $NO_2$ monitors. These ratios indicate that, by 1990, no-control scenario $NO_2$ concentrations were significantly higher than they were under the control scenario. The changes for NO are similar to those for $NO_2$.

Figure C-3. Frequency Distribution of Estimated Ratios for 1990 Control to No-control Scenario 95th Percentile 1-Hour Average $NO_2$ Concentrations, by Monitor.

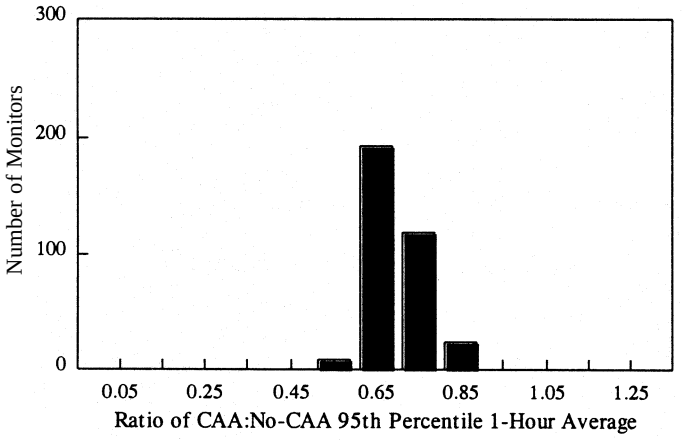


### Key caveats and uncertainties for nitrogen oxides

A number of caveats and uncertainties specific to modeling $NO_x$ should be noted. First, stack height and stack height control strategies likely to have influenced local concentrations of $SO_2$ may also have influenced local concentrations of $NO_2$ and NO. (For a fuller discussion of the stack heights issue, refer to the section "Key caveats and uncertainties for $SO_2$.") In addition, the earlier discussion of uncertainties resulting from the use of state-level emissions and the cancellation of uncertainties resulting from analyzing only differences or relative changes also applies to $NO_x$.

## Acid Deposition

The focus of air quality modeling efforts described above for carbon monoxide, sulfur dioxide, and nitrogen oxides was to estimate the change in ambient concentrations of those pollutants as a result of changes in emissions. Particularly since the emissions modeling was driven by modeled macroeconomic conditions, rather than actual historical economic activity patterns, neither the emissions inventories nor the resultant air quality conditions developed for this analysis would be expected to match historical outcomes. The need to focus on relative changes, rather than absolute predictions, becomes even more acute for estimating air quality outcomes for pollutants subject to long-range transport, chemical transformation, and atmospheric deposition. The complexity of the relationships between emissions, air concentrations, and deposition is well-described in the following paragraph from the RADM report document developed by Robin Dennis of US EPA's National Exposure Research Laboratory in support of the present analysis:

> *"Sulfur, nitrogen, and oxidant species in the atmosphere can be transported hundreds to thousands of kilometers by meteorological forces. During transport the primary emissions, $SO_2$, $NO_x$, and volatile organic emissions (VOC) are oxidized in the air or in cloud-water to form new, secondary compounds, which are acidic, particularly sulfate and nitric acid, or which add to or subtract from the ambient levels of oxidants, such as ozone. The oxidizers, such as the hydroxyl radical, hydrogen peroxide and*

[2] SAI $SO_2$, $NO_x$, and CO Report (1994), page 4-9.

*ozone are produced by reactions of VOC and $NO_x$. The sulfur and nitrogen pollutants are deposited to the earth through either wet or dry deposition creating a load of pollutants to the earth's surface... However, the atmosphere is partly cleansed of oxidants through a number of physical processes including deposition (e.g., ozone is removed by wet and dry deposition). Dry deposition occurs when particles settle out of the air onto the earth or when gaseous or fine particle species directly impact land, plants, or water or when plant stomata take up gaseous species, such as $SO_2$. In wet deposition, pollutants are removed from the atmosphere by either rain or snow. In addition, fine particles or secondary aerosols formed by the gas- and aqueous-phase transformation processes scatter or absorb visible light and thus contribute to impairment of visibility."*[3]

The complexity and nonlinearity of the relationships between localized emissions of precursors, such as $SO_2$ and VOC, and subsequent regional scale air quality and deposition effects are so substantial that the simple "roll-up" modeling methodology used for estimating local ambient concentrations of $SO_2$, $NO_x$, and CO is inadequate, even for a broad-scale, aggregate assessment such as the present study. For sulfur deposition, and for a number of other effects addressed in subsequent sections of this appendix, a regional air quality model was required. After careful review of the capabilities, geographic coverage, computing intensity, and resource requirements associated with available regional air quality models, EPA decided to use various forms of the Regional Acid Deposition Model (RADM) to estimate these effects.[4] Figure C-4 shows the geographic domain of the RADM.

## *Control scenario acid deposition profiles*

The derivation of control scenario emission inventory inputs to the RADM model is succinctly described in this excerpt from the RADM Report (1995):

*The RADM model requires a very detailed emissions inventory in both time and space. The emissions fields are also day-specific to account for the temperature effects on the volatile organics and the wind and temperature effects on the plume rise of the major point sources. At the time of the 812 retrospective study RADM runs, these inventories had been developed for 1985, using the 1985 NAPAP (National Acid Precipitation Assessment Program) inventory, and adjusted for point source*

Figure C-4. Location of the High Resolution RADM 20-km Grid Nested Inside the 80-km RADM Domain.

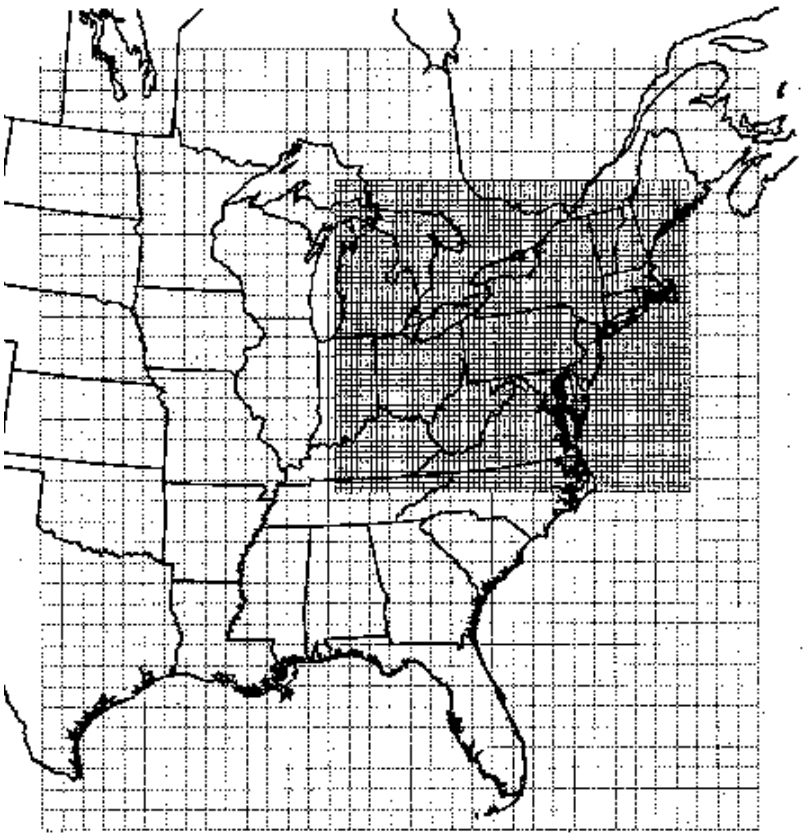

[3] Dennis, R. RADM Report (1995), p. 1.

[4] For a detailed description of the various forms of the RADM and its evaluation history, see the Dennis, R. RADM Report (1995).

*emissions to 1988 for the Eulerian Model Evaluation Field Study funded by NAPAP. These RADM emissions inventories had county-level and detailed SCC and species-level information incorporated into them to provide the 80- and 20-km detail. The 812 Study emissions are principally computed at the state level. While the 1985 812 Study emissions are close to the NAPAP inventory, they do not exactly match, nor do they have the spatial, nor economic sector, nor species detail within a state needed to run RADM. To connect the 812 Study emissions to the RADM emissions, the following approach was followed: An industry/commercial-level disaggregation (including mobile sources) was developed for the 812 emissions to allow different sectors in a state to change their emissions across time without being in lock step and the detailed NAPAP emissions for every 80- and 20-km RADM grid-cell were grouped by state to the same level of industry/commercial aggregation for an exact correspondence. Then it was assumed that the 812 Study 1985 control emissions were effectively the same as the 1985 NAPAP emissions. Relative changes in emissions between the 812 1985 control and any other scenario (e.g., 1985 no-control, or 1990 control, or 1980 no-control, etc.) were then applied to the 1985 NAPAP state-level industry/commercial groups in the appropriate 80- and 20-km grid cells. Thus, state-level emissions for each group would retain the same state-level geographic pattern in the different scenarios years, but the mix across groups could change with time. In this way, the more detailed emissions required by RADM were modeled for each scenario year using the 812 Study emissions data sets.*[5]

Figure C-5. RADM-Predicted 1990 Total Sulfur Deposition (Wet + Dry; in kg/ha) Under the Control Scenario.

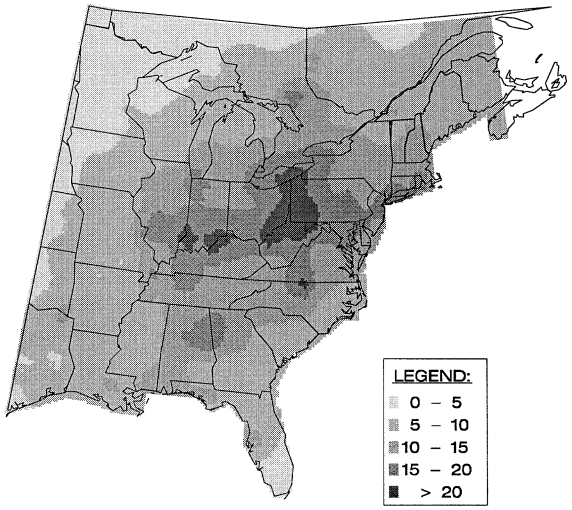


Figure C-6. RADM-Predicted 1990 Total Nitrogen Deposition (Wet + Dry; in kg/ha) Under the Control Scenario.

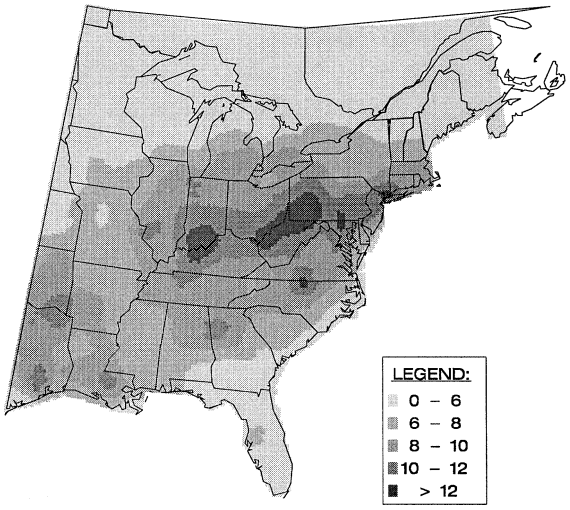


Although the focus of the present analysis is to estimate the differences between the control and no-control scenarios, it is useful to illustrate the absolute levels of acid deposition associated with the two scenarios. It is particularly important to demonstrate the initial deposition conditions to preclude possible misinterpretations of the maps showing percent change in deposition. A relatively high percentage change in a particular region, for example, may occur when initial deposition is low, even when the change in deposition is also modest. The RADM-

[5] Dennis, R. RADM Report (1995).

Figure C-7. RADM-Predicted 1990 Total Sulfur Deposition (Wet + Dry; in kg/ha) Under the No-control Scenario.

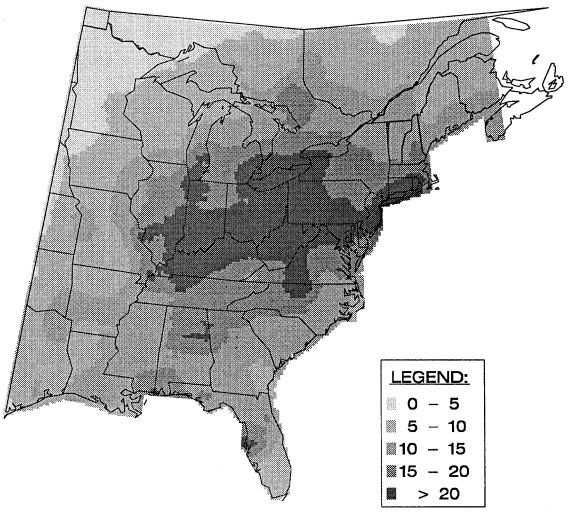


Figure C-8. RADM-Predicted 1990 Total Nitrogen Deposition (Wet + Dry; in kg/ha) Under the No-control Scenario.

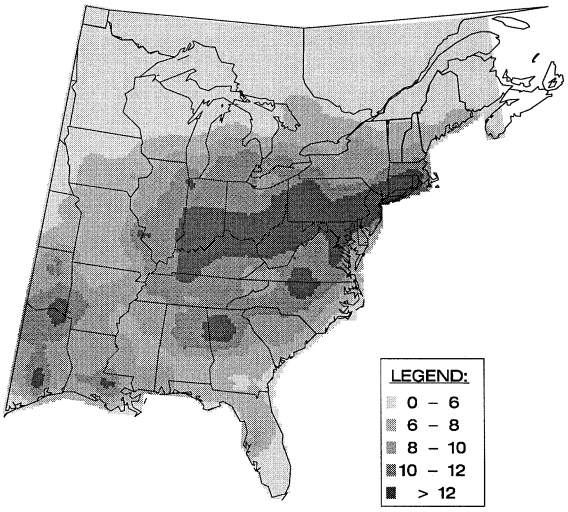


modeled 1990 control scenario wet and dry sulfur deposition pattern is shown in Figure C-5. A comparable map for nitrogen deposition is presented in Figure C-6. Maps of the RADM-predicted 1990 no-control scenario sulfur and nitrogen deposition are presented in Figures C-7 and C-8, respectively.

### *No-control scenario acid deposition profiles*

Configuration of the RADM model for the present analysis —including allocation of emission inventories to model grid cells, design of meteorological cases, treatment of biogenic versus anthropogenic emissions, and temporal, spatial, and species allocation of emissions— are described in detail in the RADM Report (1995). The remainder of this section provides a summary description of the acid deposition modeling effort.

For sulfur deposition, the RADM Engineering Model (RADM/EM), which focuses on sulfur compounds, was used to derive annual average total (wet plus dry) deposition of sulfur in kilograms sulfur per hectare (kg-S/ha) under both the control and no-control scenarios. The relative changes in annual average total sulfur deposition for each of the 80-km RADM/EM grid cells for 1975, 1980, 1985, and 1990 were then compiled.

Nitrogen deposition was calculated in a different manner. Since nitrogen effects are not included in the computationally fast RADM/EM, nitrogen deposition had to be derived from the full-scale, 15-layer RADM runs. Because of the cost and computational intensity of the 15-layer RADM, nitrogen deposition estimates were only developed for 1980 and 1990. As for sulfur deposition, the relative changes in annual average total (wet plus dry) nitrogen deposition, expressed as kg-N/ha, were calculated for each 80-km grid cell and for each of the two scenarios. It is important to note that ammonia depositin contributes significantly to total nitrogen deposition. However, the activities of sources associated with formation and deposition of ammonia, such as livestock farming and wildlife, were essentially unaffected by Clean Air Act-related control programs during the 1970 to 1990 period of this analysis. Therefore, ammonia deposition is held constant between the two scenarios.

Figure C-9. RADM-Predicted Percent Increase in Total Sulfur Deposition (Wet + Dry; in kg/ha) Under the No-control Scenario.

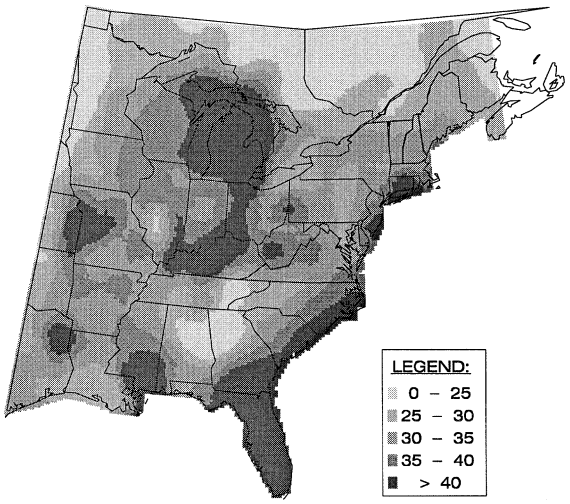


Figure C-10. RADM-Predicted Percent Increase in Total Nitrogen Deposition (Wet + Dry; in kg/ha) Under the No-control Scenario.

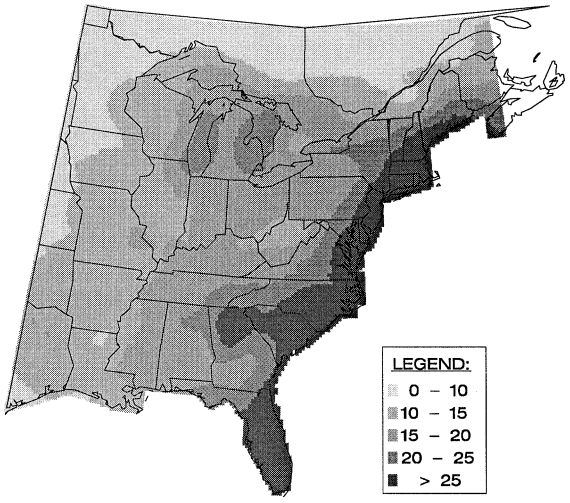


### Summary differences in acid deposition

Figure C-9 is a contour map showing the estimated percent increase in sulfur deposition under the no-control scenario relative to the control scenario for 1990. Figure C-10 provides comparable information for nitrogen deposition. These maps indicate that by 1990 acid deposition would have been significantly higher across the RADM domain under the no-control scenario.

Examination of the percent change sulfur deposition map indicates relatively large percentage changes in the upper Great Lakes and the Florida-Southeast Atlantic Coast areas. This result may appear somewhat surprising to readers familiar with the historical patterns of acid deposition. However, a review of the emission data and the control scenario sulfur deposition map reveal the reasons for this result.

First, Figure C-5 shows that control scenario deposition rates are relatively low. As described above, even a small absolute increase in deposition leads to a large percentage increase in areas with low initial rates of deposition. Second, the scenario differences in $SO_x$ emission rates for these areas were substantial. For example, 1990 no-control scenario total $SO_x$ emissions for Michigan were approximately 1.8 million tons but control scenario emissions for the same year were less than 600,000 tons; a reduction of over two-thirds. Similarly, 1990 no-control scenario emissions for Florida were over 2.3 million tons, compared to approximately 800,000 tons under the control scenario; also a reduction of about two-thirds. Almost 1 million tons of the Michigan reduction and approximately 1.3 million tons of the Florida reduction were associated with utilities. Emission reductions of these magnitudes would be expected to yield significant reductions in rates of acid deposition.

### Key caveats and uncertainties for acid deposition

Regional-scale oxidant and deposition modeling involves substantial uncertainty. This uncertainty arises from uncertainties in modeling atmospheric chemistry, incomplete meteorological data, normal seasonal and temporal fluctuations in atmospheric conditions, temporal and spatial variability

in emissions, and many other factors. Uncertainties specific to the RADM model, and this particular exercise, are discussed in detail in the RADM Report (1995). It is important, however, to highlight some of the potential sources of modeling uncertainty unique to this analysis.

The first source of uncertainty specific to this analysis is associated with the spatial and geographic disaggregation of emissions data. As discussed in the RADM Report, the RADM model requires emission inventory inputs which are highly disaggregated over both time and space. The ideal emissions inventory fed into the RADM model includes day-specific emissions to account for temperature effects on VOCs and the significance of localized meteorological conditions around major point sources. Given the broad-scale, comprehensive nature of the present study, such detailed emissions inventories were not available. However, the industry/commercial-level disaggregation approach developed for the present analysis would not be expected to introduce any systematic bias, and the contribution of this disaggregation of emissions would not be expected to contribute significantly to the overall uncertainty of the larger analysis.

The acid deposition estimates included in the present analysis are limited in that only the eastern 31 of the 48 coterminous states are covered. Although acid deposition is a problem primarily for the eastern U.S., acid deposition does occur in states west of the RADM domain. The magnitude of the benefits of reducing acid deposition in these western states is likely to be small, however, relative to the overall benefits of the historical Clean Air Act.

## Particulate Matter

Developing air quality profiles for particulate matter is significantly complicated by the fact that "particulate matter" is actually an aggregation of different pollutants with varying chemical and aerodynamic properties. Particulate species include chemically inert substances, such as wind-blown sand, as well as toxic substances such as acid aerosols; and include coarse particles implicated in household soiling as well as fine particles which contribute to human respiratory effects. In addition, emissions of both primary particulate matter and precursors of secondarily-formed particulates are generated by a wide variety of mobile and stationary sources, further complicating specification of particulate air quality models. Finally, particulate air quality models must take account of potentially significant background concentrations of atmospheric particles.

Modeling multiple species and emission sources, however, is not the only major challenge related to particulate matter which is faced in the present study. Over the 1970 to 1990 period being analyzed, understanding of the relative significance of fine versus coarse particles evolved significantly. Up until the mid-1980s, particulate air quality data were collected as Total Suspended Particulates (TSP). However, during the 1980s, health scientists concluded that small, respirable particles, particularly those with an aerodynamic diameter of less than or equal to 10 microns ($PM_{10}$), were the component of particulate matter primarily responsible for adverse human health effects. As of 1987, federal health-based ambient air quality standards for particulate matter were revised to be expressed in terms of $PM_{10}$ rather than TSP. Starting in the mid-1980s, therefore, the U.S. began shifting away from TSP monitors toward $PM_{10}$ monitors. As a result, neither TSP nor $PM_{10}$ are fully represented by historical air quality data over the 1970 to 1990 period of this analysis. Furthermore, a large number of U.S. counties have no historical PM monitoring data at all, making it difficult to estimate changes in ambient concentrations of this significant pollutant for areas containing roughly 30 percent of the U.S. population.

Given the relative significance of particulate matter to the bottom-line estimate of net benefits of the historical Clean Air Act, it was important to develop methodologies to meet each of these challenges. The methodologies developed and data used are described primarily in the two supporting documents SAI PM Report (1992) and SAI PM Report (1995).[6] To summarize the overall approach, historical TSP data were broken down into principal component species, including primary particulates, sulfates, nitrates, organic particulates, and background particulates. Historical data were used for the control scenario. To derive the no-control profiles, the four non-background components were scaled up based on corresponding no-control to control scenario ratios of emissions and/or modeled atmospheric concentrations. Specifically, the primary particulate component was scaled up by the ratio of no-control to control emissions of PM.

[6] In addition, SAI memoranda and reports which supplement the results and methodologies used in this analysis are included in the references.

Organic constituents were scaled up by the ratio of no-control to control VOC emissions. In the eastern 31 states where RADM sulfate and nitrate data were available, values for $SO_4$ and $NO_3$ from an appropriate RADM grid cell were assigned to the relevant county and used to scale these components of PM. For the western states not covered by RADM, sulfates were scaled up by the change in $SO_2$ emissions and nitrates were scaled up the change in $NO_x$ emissions. No-control scenario profiles were then constructed by adding these scaled components to background concentrations.

To resolve the problem of variable records of TSP and $PM_{10}$ data, both TSP and $PM_{10}$ profiles were generated for the entire 20 year period. Missing early year data for $PM_{10}$ were derived by applying region-specific, land use category-specific $PM_{10}$ to TSP ratios to the historical TSP data. Missing recent year TSP data were derived for those areas where $PM_{10}$ monitors replaced TSP monitors by applying the reciprocal of the relevant $PM_{10}$ to TSP ratio. The methodology is described in detail in the SAI PM Report (1995).

In addition, to increase the geographic coverage of estimates of air quality, an interpolation methodology[7] was developed to predict air quality for the control scenario in counties without measured data. PM concentrations were estimated by first estimating the components of PM (i.e., sulfate, nitrate, and organic particulate, and primary particulate). The methodology for developing the concentrations of components within a county differed depending upon whether the county was within or outside the RADM domain.

For those counties within the RADM domain, the RADM modeled concentrations for 1980 and 1990 were used to predict sulfate air quality. Relationships based on linear regressions that related 1980 and 1990 RADM sulfate concentrations to estimated sulfate particulate concentrations were calculated for counties with AIRS data. Sulfate particulate concentrations were then calculated for all counties in the domain by applying the regression results to the RADM grid cell concentration located over the county center. Statewide average nitrate, VOC, and primary particulate concentrations were calculated from measured ambient TSP and $PM_{10}$ to describe these constituents in counties without data. Control scenario PM profiles were developed by adding the RADM-estimated sulfate particulate levels to the statewide average nitrate, VOC, and primary particulate levels, and background.

For counties outside the RADM domain, an alternate procedure was used. Using the primary and secondary particulate estimates for counties with data, statewide average sulfate, nitrate, VOC, and primary particulate concentrations were determined. Control scenario $PM_{10}$ was predicted by adding the statewide averages of all primary and secondary particulate, and background. Using this method, all counties that did not have monitors and are in the same state are assigned the same PM concentration profiles. These interpolated results are clearly less certain than results based on actual historical monitoring data and are therefore presented separately.

### *Control scenario particulate matter profiles*

The number of TSP monitors peaked in 1977 and declined throughout the 1980s. Table C-6 summarizes the daily (i.e., 24-hour average) TSP monitoring data used as the basis for development of the control scenario air quality profiles. Most of the TSP and $PM_{10}$ monitors collected samples every six days (i.e., 61 samples per year).

Daily $PM_{10}$ data were also collected for each year between 1983 and 1990. Table C-7 summarizes the daily $PM_{10}$ monitoring data used for the control scenario air quality profiles.

Table C-6. Summary of TSP Monitoring Data.

| Year | Number of Monitors | Number of Counties | Number of Samples | Mean Number of Samples per Monitor |
|---|---|---|---|---|
| **1970** | 751 | 245 | 56,804 | 76 |
| **1975** | 3,467 | 1,146 | 221,873 | 64 |
| **1980** | 3,595 | 1,178 | 234,503 | 65 |
| **1985** | 2,932 | 1,018 | 189,344 | 65 |
| **1990** | 923 | 410 | 59,184 | 64 |

Data Source: SAI PM Report (1995).

[7] The interpolation methodology is described in detail in SAI, 1996. Memo from J. Langstaff to J. DeMocker. PM Interpolation Methodology for the section 812 retrospective analysis. March 1996.

Table C-7. Summary of $PM_{10}$ Monitoring Data.

| Year | Number of Monitors | Number of Counties | Number of Samples | Mean Number of Samples per Monitor |
|---|---|---|---|---|
| **1985** | 303 | 194 | 22,031 | 73 |
| **1990** | 1,249 | 556 | 98,904 | 79 |

Data Source: SAI PM Report (1995).

Further speciation of TSP and $PM_{10}$ air quality data serves two purposes in the present analysis. First, speciation of TSP into $PM_{10}$ and other fractions allows derivation of $PM_{10}$:TSP ratios. Such ratios can then be used to estimate historical $PM_{10}$ for those years and monitors which had TSP data but no $PM_{10}$ data. The reciprocal ratio is also applied in this analysis to expand 1985 and 1990 TSP data to cover those areas which monitored $PM_{10}$ but not TSP. The second purpose served by speciation of particulate data is, as described earlier, to provide a basis for scaling up concentrations of each species to derive no-control scenario TSP and $PM_{10}$ profiles.

To break the TSP and $PM_{10}$ data down into component species, speciation factors were applied to the PM fractions with aerodynamic diameters below 2.5 microns ($PM_{2.5}$) and from 2.5 to 10 microns ($PM_{10}$). The $PM_{2.5}$ speciation factors were drawn from a National Acid Precipitation Assessment Program (NAPAP) report on visibility which reviewed and consolidated speciation data from a number of studies.[8] These factors are presented in Table C-8. In the table, fine particle concentrations are based on particle mass measured after equilibrating to a relative humidity of 40 to 50 percent; and organics include fine organic carbon.

To develop speciation factors for coarser particles (i.e., in the $PM_{2.5}$ to $PM_{10}$ range), SAI performed a review of the available literature, including Conner et al. (1991), Wolff and Korsog (1989), Lewis and Macias (1980), Wolff et al. (1983), Wolff et al. (1991), and Chow et al. (1994).[9] These speciation factors are summarized in Table C-9. Data were too limited to allow differentiation between urban and rural locations for coarser particles.

The TSP and $PM_{10}$ control scenario profiles developed based on this methodology are available on diskette, under the filenames listed in Table C-10.

### No-control scenario particulate matter profiles

To derive the no-control TSP and $PM_{10}$ air quality profiles, individual component species were adjusted to reflect the relative change in emissions or, in the case of sulfates and nitrates in the eastern U.S., the relative change in modeled ambient concentration. The following excerpt from the SAI PM Report (1995) describes the specific algorithm used:[10]

> *"For the retrospective analysis, the no-CAA scenario TSP and $PM_{10}$ air quality was estimated by means of the following algorithm:*
>
> - *Apportion CAA scenario TSP and $PM_{10}$ to size categories and species;*
> - *Adjust for background concentrations;*
> - *Use a linear scaling to adjust the non-background portions of primary particulates, sulfate, nitrate, and organic components based on emissions ratios of PM, $SO_2$, $NO_x$ and VOC, and Regional Acid Deposition Model (RADM) annual aggregation results for $SO_4$ and $NO_3$;*
> - *Add up the scaled components to estimate the no-CAA scenario TSP and $PM_{10}$ concentrations."*

The specific procedures and values used for the linear rollback, speciation, fine to coarse particle ratio, scaling, and background adjustment steps are described in detail in the SAI PM report (1995).[11] Table C-11 lists the names of the electronic data files containing the TSP and $PM_{10}$ profiles for the no-control scenario.

[8] J. Trijonis, "Visibility: Existing and Historical Conditions--Causes and Effects," NAPAP Report 24, 1990.

[9] This literature review, and complete citations of the underlying studies, are presented in the SAI PM Report (1995), pp. 4-2 to 4-6 and pp. R-1 to R-2, respectively.

[10] SAI PM Report (1995), p. 5-1.

[11] SAI PM Report (1995), pp. 5-2 to 5-15.

Table C-8. Fine Particle ($PM_{2.5}$) Chemical Composition by U.S. Region.

| Component | Units | Number of Data Sets | Arithmetic Mean | Range of Values |
|---|---|---|---|---|
| **RURAL EAST** | | | | |
| Fine particle concentration | µg/m3 | 19 | 18 | 6 - 46 |
| Ammonium sulfate | % Fine particles | 19 | 52 | 41 - 66 |
| Ammonium nitrate | % Fine particles | 3 | 1 | 1 |
| Organics | % Fine particles | 5 | 24 | 9 - 34 |
| **URBAN EAST** | | | | |
| Fine particle concentration | µg/m3 | 3 | 36 | 29 - 43 |
| Ammonium sulfate | % Fine particles | 3 | 55 | 53 - 57 |
| Ammonium nitrate | % Fine particles | 2 | 1 | 1 |
| Organics | % Fine particles | 2 | 24 | 15 - 32 |
| **RURAL WEST** | | | | |
| Fine particle concentration | µg/m3 | 25 | 5 | 1 - 11 |
| Ammonium sulfate | % Fine particles | 25 | 35 | 15 - 56 |
| Ammonium nitrate | % Fine particles | 17 | 4 | 1 - 17 |
| Organics | % Fine particles | 25 | 27 | 14 - 41 |
| **URBAN WEST** | | | | |
| Fine particle concentration | µg/m3 | 16 | 35 | 13 - 74 |
| Ammonium sulfate | % Fine particles | 16 | 16 | 3 - 35 |
| Ammonium nitrate | % Fine particles | 14 | 15 | 2 - 37 |
| Organics | % Fine particles | 16 | 42 | 25 - 79 |

Data Sources: SAI PM Report (1995); and J. Trijonis, *"Visibility: Existing and Historical Conditions--Causes and Effects,"* NAPAP Report 24, 1990.

### *Summary differences in particulate matter air quality*

Figure C-11 provides one indication of the estimated change in particulate matter air quality between the control and no-control scenarios. Specifically, the graph provides data on the estimated ratios of 1990 control to no-control scenario annual mean TSP concentrations in monitored counties. The X-axis values represent the mid-point of the ratio interval bin, and the Y-axis provides the number of counties falling into each bin. Figure C-11 indicates that annual average TSP concentrations would have been substantially higher in monitored counties under the no-control scenario.

### *Key caveats and uncertainties for particulate matter*

There are several important caveats and uncertainties associated with the TSP and $PM_{10}$ air quality profiles developed for this study. Although further

Table C-9. Coarse Particle ($PM_{2.5}$ to $PM_{10}$) Chemical Composition by U.S. Region.

| Component | Units | Number of Data Sets | Arithmetic Mean | Range of Values |
|---|---|---|---|---|
| **EAST** | | | | |
| Coarse particle concentration | µg/m³ | 1 | 5.5 | 5.5 |
| Ammonium sulfate | % Coarse particles | 3 | 3 | 1 - 4 |
| Ammonium nitrate | % Coarse particles | 1 | 4 | 4 |
| Organics | % Coarse particles | 2 | 10 | 7 - 13.8 |
| **WEST** | | | | |
| Coarse particle concentration | µg/m³ | 18 | 24 | 7.7 - 56.7 |
| Ammonium sulfate | % Coarse particles | 18 | 6 | 2.1 - 10.39 |
| Ammonium nitrate | % Coarse particles | 18 | 18 | 2.33-28.52 |
| Organics | % Coarse particles | 18 | 14 | 8.41-25.81 |

Data Source: SAI PM Report (1995).

Table C-10. PM Control Scenario Air Quality Profile Filenames.

| Component | Indicator | Filename |
|---|---|---|
| **TSP** | Annual Mean | TSPCMEAN.DAT |
| **TSP** | 2nd Highest Daily | TSPCHI2.DAT |
| **TSP** | (X)th Percentile | TSPC(X).DAT |
| **$PM_{10}$** | Annual Mean | PM10CMEA.DAT |
| **$PM_{10}$** | 2nd Highest Daily | PM10CHI2.DAT |
| **$PM_{10}$** | (X)th Percentile | PM10C(X).DAT |

Note: "(X)" refers to percentiles from 5 to 95, indicating 19 percentile data files available for TSP and 19 files available for $PM_{10}$; for example, the filename for the 50th percentile TSP air quality data profile for the control scenario is named TSPC50.DAT.

Table C-11. PM No-Control Scenario Air Quality Profile Filenames.

| Component | Indicator | Filename |
|---|---|---|
| TSP | Annual Mean | TSPCNMEA.DAT |
| TSP | 2nd Highest Daily | TSPNCHI.DAT |
| TSP | (X)th Percentile | TSPNC(X).DAT |
| $PM_{10}$ | Annual Mean | PM10NCME.DAT |
| $PM_{10}$ | 2nd Highest Daily | PM10NCHI.DAT |
| $PM_{10}$ | (X)th Percentile | PM10NC(X).DAT |

Note: "(X)" refers to percentiles from 5 to 95, indicating 19 percentile-based data files available for TSP and 19 similar files available for $PM_{10}$; for example, the filename for the 50th percentile TSP air quality data profile for the no-control scenario is named TSPNC50.DAT.

reductions in these uncertainties were not possible for this study given time and resource limitations, the relative importance of particulate matter reduction contributions towards total benefits of the Clean Air Act highlights the importance of these uncertainties.

A number of uncertainties were introduced in the process of speciating and rolling up individual components of particulate matter. First, temporal and spatial variability in the size and chemical properties of particulate emissions are substantial. These characteristics change from day to day at any given location. Second, using changes in proxy pollutant emissions, such as using $SO_2$ as a surrogate for $SO_4$ in the western states, to roll up individual PM components may introduce significant uncertainty. Third, even assuming a satisfactorily high degree of correlation between target and surrogate pollutants, relying on predicted changes in emissions at the state level further compounds the uncertainty. Finally, and perhaps most important, using $PM_{10}$ to TSP ratios derived from late 1980s monitoring data may lead to significant underestimation of reductions in fine particulates achieved in earlier years. This is because historical Clean Air Act programs focused extensively on controlling combustion sources of fine particulates. As a result, the share of TSP represented by $PM_{10}$ observed in the late 1980s would be lower due to implementation of controls on combustion sources. This would lead, in turn, to underestimation of baseline $PM_{10}$ concentrations, as a share of TSP, in the 1970s and early 1980s. If baseline $PM_{10}$ concentrations in these early years are underestimated, the reductions in $PM_{10}$ estimated by linear scaling would also be underestimated.[12]

Figure C-11. Distribution of Estimated Ratios for 1990 Control to No-control Annual Mean TSP Concentrations, by Monitored County.

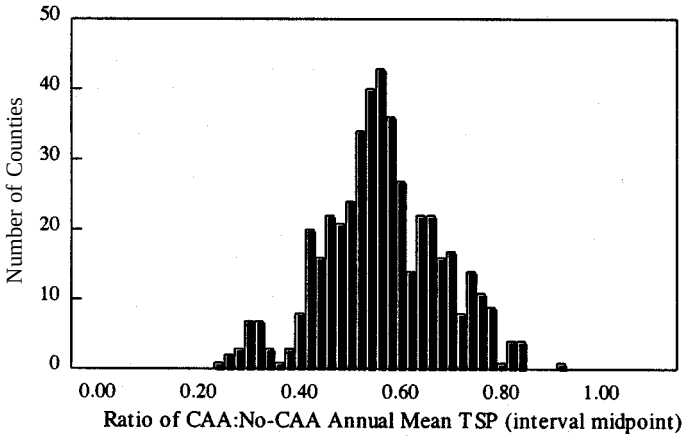


## Ozone

Nonlinear formation processes, long-range atmospheric transport, multiple precursors, complex atmospheric chemistry, and acute sensitivity to meteorological conditions combine to pose substantial difficulties in estimating air quality profiles for ozone. Even in the context of an aggregated, national study such as this, the location-specific factors controlling ozone formation preclude the use of roll-up modeling based on proxy pollutants or application of state-wide or nation-wide average conditions. Such simplifications would yield virtually meaningless results for ozone.

Ideally, large-scale photochemical grid models — such as the Urban Airshed Model (UAM)— would be used to develop control and no-control scenario estimates for ozone concentrations in rural and urban areas. Such models provide better representations of the effects of several important factors influencing air quality projections such as long-range atmospheric transport of ozone. However, the substantial computing time and data input requirements for such models precluded their use for this study.[13] Instead, three sepa-

[12] See SAI PM Report (1995), p. 5-9.

[13] For a description of the extensive data inputs required to operate UAM, see SAI Ozone Report (1995), p. 1-1.

Table C-12. Urban Areas Modeled with OZIPM4.

| | | |
|---|---|---|
| Albany, NY | Fort Wayne, IN | Owensboro, KY |
| Albuquerque, NM | Grand Rapids, MI | Parkersburg, WV |
| Allentown, PA-NJ | Greeley, CO | Pascagoula, MS |
| Altoona, PA | Green Bay, WI | Pensacola, FL |
| Anderson, IN | Greensboro, NC | Peoria, IL |
| Appleton, WI | Greenville, SC | Philadelphia, PA |
| Asheville, NC | Harrisburg, PA | Phoenix, AZ |
| Atlanta, GA | Hartford, CT | Portland, OR |
| Atlantic City, NJ | Houston, TX | Portsmouth, NH |
| Auburn, ME | Huntington, WV-KY | Raleigh, NC |
| Augusta, GA-SC | Huntsville, AL | Reading, PA |
| Austin, TX | Indianapolis, IN | Reno, NV |
| Baltimore, MD | Iowa City, IA | Richmond, VA |
| Baton Rouge, LA | Jackson, MS | Roanoke, VA |
| Beaumont, TX | Jacksonville, FL | Rochester, NY |
| Bellingham, WA | Janesville Rock Co, WI | Rockford, IL |
| Billings, MT | Johnson City, TN-VA | Sacramento, CA |
| Birmingham, AL | Johnstown, PA | Salt Lake City, UT |
| Boston, MA | Kansas City, MO | San Antonio, TX |
| Boulder, CO | Knoxville, TN | San Diego, CA |
| Canton, OH | Lafayette, IN | San Francisco, CA |
| Cedar Rapids, IA | Lafayette, LA | San Joaquin Valley, CA |
| Champaign, IL | Lake Charles, LA | Santa Barbara, CA |
| Charleston, SC | Lancaster, PA | Sarasota, FL |
| Charleston, WV | Lansing, MI | Scranton, PA |
| Charlotte, NC | Las Cruces, NM | Seattle, WA |
| Chattanooga, TN-GA | Las Vegas, NV | Sheboygan, WI |
| Chicago, IL | Lexington, KY | Shreveport, LA |
| Cincinnati, OH | Lima, OH | South Bend, IN |
| Cleveland, OH | Little Rock, AR | Springfield, IL |
| Colorado Springs, CO | Longview, TX | Springfield, MO |
| Columbia, SC | Los Angeles, CA | Springfield, OH |
| Columbus, GA-AL | Louisville, KY | St Louis, MO |
| Columbus, OH | Lynchburg, VA | Steubenville, OH-WV |
| Corpus Christi, TX | Medford, OR | Syracuse, NY |
| Cumberland, MD-WV | Memphis, TN | Tallahassee, FL |
| Dallas, TX | Miami, FL | Tampa, FL |
| Davenport, IA-IL | Minneapolis, MN-WI | Terre Haute, IN |
| Decatur, IL | Mobile, AL | Toledo, OH |
| Denver, CO | Monroe, LA | Tucson, AZ |
| Detroit, MI | Montgomery, AL | Tulsa, OK |
| El Paso, TX | Nashville, TN | Utica-Rome, NY |
| Erie, PA | New Orleans, LA | Ventura County, CA |
| Eugene, OR | New York, NY | Victoria, TX |
| Evansville, IN | Norfolk, VA | Washington, DC |
| Fayetteville, NC | Oklahoma City, OK | Wheeling, WV-OH |
| Flint, MI | Omaha, NE-IA | Wichita, KS |
| Fort Collins, CO | Orange Co, CA | York, PA |
| Fort Smith, AR-OK | Orlando, FL | Youngstown, OH-PA |

rate modeling efforts were conducted to provide urban and rural ozone profiles for those areas of the lower 48 states in which historical ozone changes attributable to the Clean Air Act may be most significant.

First, for urban areas the Ozone Isopleth Plotting with Optional Mechanisms-IV (OZIPM4) model was run for 147 urban areas. Table C-12 lists the urban areas modeled with OZIPM4. Although it requires substantially less input data than UAM, the OZIPM4 model provides reasonable evaluations of the relative reactivity of ozone precursors and ozone formation mechanisms associated with urban air masses.[14] Three to five meteorological episodes were modeled for each

[14] See SAI Ozone Report (1995), p. 1-1.

of the 147 urban areas; and for each of these, four model runs were performed to simulate the 1980 and 1990 control and no-control scenarios. The outputs of these model runs were peak ozone concentrations for each of the target year-scenario combinations. The differentials between the control and no-control scenario outputs were averaged over meteorological episodes and then applied to scale up historical air quality at individual monitors to obtain no-control case profiles. As for the other pollutants, the control scenario profiles were derived by fitting statistical distributions to actual historical data for individual monitors.

Second, the 15-layer RADM runs for 1980 and 1990 were used to estimate the relative change in rural ozone distributions for the eastern 31 states. In addition, a limited number of 20-km grid cell high-resolution RADM runs were conducted to benchmark the 15-layer, 80-km RADM median ozone response and to estimate high ozone response. The relative changes in modeled median and 90th percentile rural ozone were then assumed to be proportional to the changes in, respectively, the median and 90th percentile ozone concentrations. The domain of the high-resolution RADM is shown in Figure C-4 and the general RADM domain is shown in Figure C-12.

Finally, the SARMAP Air Quality Model (SAQM) was run for EPA by the California Air Resources Board (CARB) to gauge the differences in peak ozone concentrations in key California agricultural areas for 1980 and 1990. No-control profiles were developed for ozone monitors in these areas by assuming the relative change in peak ozone concentration also applies to the median of the ozone distribution. The domain of the SAQM is shown in Figure C-12.

Figure C-12. RADM and SAQM Modeling Domains, with Rural Ozone Monitor Locations.

### Control scenario ozone profiles

For ozone, air quality profiles were developed from historical AIRS data and calculated for individual monitors based on 1, 2, 6, 12, and 24 hour averaging times. Profiles based on the daily maximum concentrations for these averaging times were also calculated. Given the significance of seasonal and diurnal ozone formation, twelve separate profiles of hourly ozone distributions were also developed for six 2-month periods and for daytime and nighttime hours. The 2-month periods are January-February, March-April, and so forth. The diurnal/nocturnal profiles are divided at 7 A.M. and 7 P.M. Local Standard Time. All of these profiles are based on constructing 1, 2, 6, 12, and 24-hour moving average profiles from the hourly ozone data from each monitor.[15] A two-parameter gamma distribution is then fitted to characterize each of these air quality profiles.[16] The functional form of the gamma distribution, the basis for deriving the monitor-specific values for mean and variance, and an analysis of the goodness of fit to the data are presented in the SAI Ozone Report (1995).

Table C-13 summarizes the ozone monitoring data used as the basis for the control scenario profiles. The distribution of these monitors among urban, suburban, and rural locations is presented in Table C-2 of the SAI Ozone Report (1995).

Table C-13. Summary of Ozone Monitoring Data.

| Year | Number of Monitors | Number of Counties |
|---|---|---|
| 1970 | 1 | 1 |
| 1975 | 467 | 240 |
| 1980 | 791 | 415 |
| 1985 | 719 | 415 |
| 1990 | 834 | 477 |

Data Source: SAI Ozone Report (1995).

Given the substantial number of alternative air quality profiles for ozone, approximately 20 high-density disks are required to hold the profiles, even in compressed data format. Resource limitations therefore preclude general distribution of the actual profiles. As discussed in the caveats and uncertainties subsection below, however, the substantial uncertainties associated with model results for any given area preclude application of these profiles in contexts other than broad-scale, aggregated assessments such as the present study. The historical ozone monitoring data used as the basis for this study are, nevertheless, available through EPA's Aerometric Information Retrieval System (AIRS).

### No-control scenario ozone profiles

The specific modeling methodologies for the OZIPM4 runs —including emissions processing, development of initial and boundary conditions, meteorological conditions, simulation start and end times, organic reactivity, and carbon fractions— are described in detail in the SAI Ozone Report (1995). Assumptions and modeling procedures not otherwise described in the SAI report were conducted in accordance with standard EPA guidance.[17]

Similarly, the RADM modeling methodology used to estimate changes in day-time rural ozone distributions in the eastern 31 states are described in detail in the RADM Report (1995). The referenced report also provides complete citations of the literature associated with development, standard application procedures, and evaluation of RADM by the National Acid Precipitation Assessment Program (NAPAP).

To derive the no-control scenario results for key California agricultural areas, the California Air Resources Board and US EPA's Region 9 office agreed to conduct three runs of the SAQM. For the 1990 control scenario, the 1990 SARMAP base case scenario adopted for California State Implementation Plan modeling was adopted.[18] Derivation of 1990

[15] For the nighttime profiles, only 1, 2, 6, and 12-hour averaged concentrations are derived.

[16] Normal and lognormal distributions were also developed and tested for goodness of fit; however, the gamma distribution provided a better representation of the concentration distribution. See SAI Ozone Report (1995), page 4-2.

[17] US EPA, Office of Air Quality Planning and Standards, "*Procedures for Applying City-Specific EKMA*," EPA-450/4-89-012, 1989.

[18] Documentation of the SARMAP Air Quality Model and the SARMAP 1990 base case can be found in the SAQM references listed at the end of this appendix.

no-control and 1980 control and no-control scenarios was based on adjusting the aggregate mobile, point, and area source VOC and $NO_x$ emissions associated with each of these cases. For example, the 1980 no-control results were derived by, first, multiplying the 1990 SARMAP base case mobile source VOC emissions by the ratio of 1980 no-control scenario to 1990 control scenario mobile source VOC emissions derived for the present study. Similar adjustments were made for point and area sources, and for $NO_x$. The SAQM was then re-run holding fixed all other conditions associated with the 1990 SARMAP base case, including meteorology, activity patterns, and other conditions. The specific emission ratios used to modify the 1990 SARMAP base case are presented in Table C-14. The ratios themselves were derived by adding on-highway and off-highway emissions to represent the mobile source category; adding utility, industrial process, and industrial combustion emissions to represent point sources; and using commercial/residential emissions to represent area sources. The no-control scenarios were then derived by adjusting the peak and median of the control scenario ozone distribution based on the ratio of SARMAP-predicted peak ozone concentrations under the control and no-control scenarios.

Table C-14. Apportionment of Emissions Inventories for SAQM Runs.

| | Source Category | 1980 Control to 1990 Control Ratio | 1980 No-Control to 1990 Control Ratio | 1990 No-Control to 1990 Control Ratio |
|---|---|---|---|---|
| VOC | Mobile | 1.344 | 1.955 | 3.178 |
| | Area | 0.820 | 0.901 | 1.106 |
| | Point | 1.284 | 1.439 | 1.232 |
| $NO_x$ | Mobile | 1.042 | 1.148 | 1.677 |
| | Area | 0.731 | 0.738 | 1.058 |
| | Point | 0.987 | 1.339 | 1.159 |

The relative results of the control and no-control scenario runs of the OZIPM4, RADM, and SAQM models were then used to derive the no-control case air quality profiles. For the urban monitors relying on OZIPM4 results, only ozone-season daytime concentrations could be calculated directly from OZIPM4 results. This is because OZIPM4 provides only the maximum hourly ozone concentration. However, to estimate all the various physical consequences of changes in ambient ozone concentrations, the current study requires estimation of the shift in the entire distribution of ozone concentrations. Since it is daytime ozone season concentrations which are most sensitive to changes in VOC and $NO_x$ emissions, the predicted shifts in the most important component of the ozone concentration distribution are reasonably well-founded. The method adopted for this analysis involved applying the no-control to control peak concentration ratio to all concentrations in the distribution down to a level of 0.04 ppm. The 0.04 ppm level is considered at the high end of hypothetical ambient ozone concentrations in the absence of all anthropogenic ozone precursor emissions. A ratio of 1.0 is used for ozone concentrations at or near zero. The methodology is described in more detail in the SAI Ozone Report (1995) on page 4-6.

Estimating changes in rural ozone concentrations is required primarily for estimating effects on agricultural crops, trees, and other vegetation. For this reason, only the differences in daytime, growing season ozone concentrations are derived for the present study. As described in detail in the SAI Ozone Report (1995) on page 4-7, the no-control rural ozone profiles are calculated by, first, taking the ratio of the average daytime growing season ozone concentrations simulated by RADM or SAQM (whichever is relevant for that monitor). The ratio of no-control to control scenario average ozone concentration is then applied to all the hourly concentrations from that monitor.

Profiles based on 1, 2, 6, 12, and 24-hour averages are then calculated for the control case; and averages for daytime hours are calculated for the no-control case.[19] Even though the control and no-control scenario off-season profiles are held constant, profiles for the no-control scenario are developed for all months of the year since the ozone season varies throughout the country.

### *Summary differences in ozone air quality*

Figure C-13 presents a summary of the results of the 1990 OZIPM4 results for all 147 of the modeled urban areas. Specifically, the graph depicts a frequency distribution of the ratio of control to no-control scenario peak ozone. While the vast majority of simulated peak ozone concentration ratios fall below 1.00, eight urban areas show lower simulated peak ozone for the no-control scenario than for the control scenario. For these eight urban areas, emissions of precursors were higher under the no-control scenario; however, the high proportion of ambient $NO_x$ compared to ambient non-methane organic compounds (NMOCs) in these areas results in a decrease in net ozone production when $NO_x$ emissions increase. Figures C-14 and C-15 present frequency distributions for control to no-control ratios of average ozone-season daytime ozone concentrations at rural monitors as simulated by RADM and SAQM, respectively.

These figures indicate that, by 1990, no-control scenario ozone concentrations in the modeled areas would have been generally higher in both urban and rural areas. Rural area concentrations differences are not as great as urban area differences due to (a) the differentially greater effect of CAA emission controls in high population density areas, and (b) potential differences in the models used for urban and rural areas.

Ozone reductions in both rural and urban areas projected in this analysis are not as proportionally large as the estimated reductions in emissions of ozone precursors for at least four reasons. First, current knowledge of atmospheric photochemistry suggests that ozone reductions resulting from emissions changes will be proportionally smaller than the emissions reductions. Second, biogenic emissions of VOCs, an important ozone precursor, are significant and are held constant for the control and no-control scenarios of this analysis. Biogenic emissions are important because they contribute roughly half of the total

Figure C-13. Distribution of Estimated Ratios for 1990 Control to No-control OZIPM4-Simulated 1-Hour Peak Ozone Concentrations, by Urban Area.

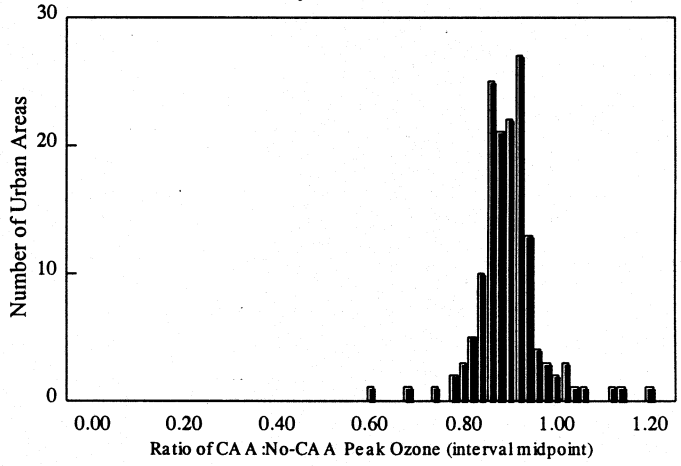


Figure C-14. Distribution of Estimated Ratios for 1990 Control to No-control RADM-Simulated Daytime Average Rural Ozone Concentrations, by RADM Grid Cell.

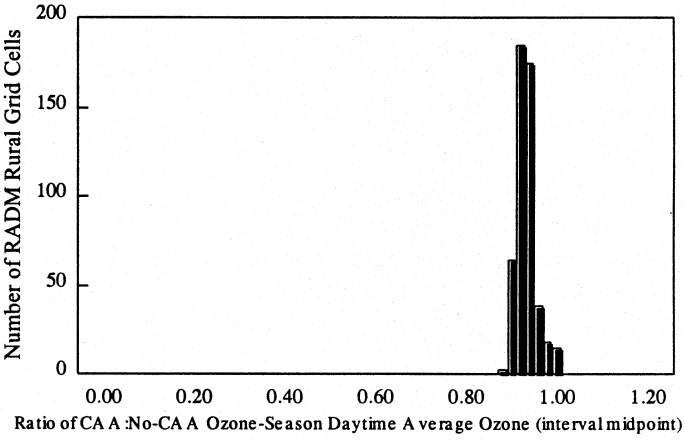


Figure C-15. Distribution of Estimated Ratios for 1990 Control to No-control SAQM-Simluated Daytime Average Ozone Concentrations, by SAQM Monitor.

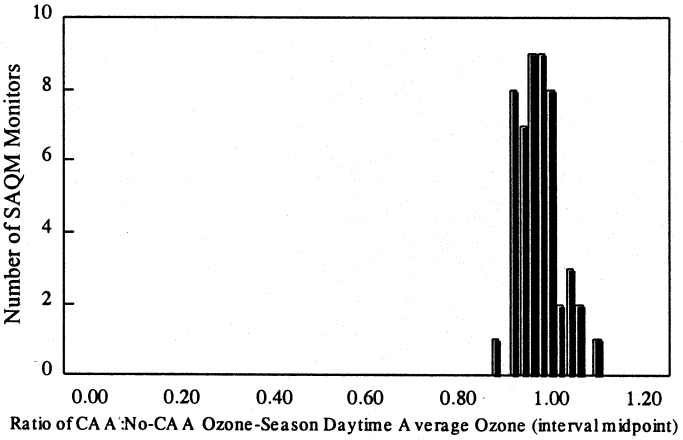


[19] The no-control scenario nighttime profiles are assumed to be the same as the control scenario profiles.

(manmade plus natural) VOC emissions nationwide. Due to this abundance of VOC loading and the inherent nonlinearity of the ozone-precursor response system,[20] historical reductions in anthropogenic VOC emissions can yield minimal reductions in ozone, especially in rural environments. Third, this rural effect also influences urban areas receiving substantial ozone transported in from surrounding areas. Consequently, the effect of emission controls placed in urban areas often is reduced since much of the urban area ozone is imported. Thus, the problem is truly regionalized given the importance of transport, biogenic emissions and associated urban-rural interactions, all contributing toward a relatively non-responsive atmospheric system.[21] Finally, physical process characterizations within OZIPM4 are severely limited and incapable of handling transport, complex flow phenomena, and multi-day pollution events in a physically realistic manner. Consequently, it is possible that the OZIPM4 method used herein produces negative bias tendencies in control estimations. Additional discussion of uncertainties in the ozone air quality modeling is presented in the following section.

### Key caveats and uncertainties for ozone

There are a number of uncertainties in the overall analytical results of the present study contributed by the ozone air quality modeling in addition to the potential systematic downward bias discussed above. First, there are substantial uncertainties inherent in any effort to model ozone formation and dispersion. These uncertainties are compounded in the present study by the need to perform city-specific air quality modeling using OZIPM4, which is less sophisticated than an Eulerian model such as the Urban Airshed Model. However, while the absolute ozone predictions for any given urban area provided by OZIPM4 may be quite uncertain, the process of aggregating results for a number of cities and meteorological episodes should significantly reduce this uncertainty.[22] Urban areas for which ozone changes may be overpredicted are offset to some degree by urban areas for which the change in ozone concentrations may be underpredicted. In weighing the significance of this source of uncertainty, it is important to consider the central purpose of the present study, which is to develop a reasonable estimate of the overall costs and benefits of all historical Clean Air Act programs. All analyses are based on relative modeled results, and ratios of the model predictions for the control and no-control scenarios, rather than the absolute predictions. As a result of this, the effect of any bias in the model predictions is greatly reduced due to partial cancellation.

Additional uncertainty is contributed by other limitations of the models, the supporting data, and the scope of the present analysis. Relying on linear interpolation between 1970 and modeled 1980 results to derive results for 1975, and between modeled results for 1980 and 1990 to derive results for 1985, clearly adds to the uncertainty associated with the RADM-based rural ozone estimates. Assuming that changes in peak concentration predicted by OZIPM4 and SAQM can be applied to scale hourly ozone values throughout the concentration distribution also contributes to uncertainty. Resource and model limitations also required that night-time ozone concentrations be held constant between the scenarios. This leads to an underestimation of the night-time component of ozone transport. Finally, changes in rural ozone in areas not covered by RADM or SAQM could not be estimated. As a result, potentially significant changes in ambient ozone in other major agricultural areas, such as in the mid-west, could not be developed for this analysis. The Project Team considered using an emissions scaling (i.e., a roll-back) modeling strategy to develop crude estimates of the potential change in rural ozone concentrations in monitored areas outside the RADM and SAQM domains. However, the Project Team concluded that such estimates would be unreliable due to the nonlinear effect on ozone of precursor emission changes. Furthermore, the team concluded that baseline levels of ozone and changes in precursor emissions in these areas are relatively low. The decision not to spend scarce project resources on estimating ozone changes in these rural areas is further supported by the relatively modest change in rural ozone concentrations estimated within the RADM and SAQM domains.

[20] Nonlinear systems are those where a reduction in precursors can result in a wide range of responses in secondary pollutants such as ozone. Ozone response often is "flat" or nonresponsive to reductions of VOCs in many rural areas with significant natural VOC emissions. Also, ozone can increase in response to increases in $NO_x$ emissions in certain localized urban areas.

[21] Both the 1990 CAA and EPA's and the National Academy of Science's Section 185B Report to Congress recognized the consequences of biogenics, transport and the need to conduct regionalized assessments, as reflected in organizational structures such as the Ozone Transport Commission and the North American Research Strategy for Tropospheric Ozone (NARSTO).

[22] Note that aggregating individual urban area results may reduce the effect of uncertainty in individual city projections (i.e., overestimated cities would offset underestimated cities). However, aggregation of individual urban area results would not reduce potential errors caused by systematic biases which arise due to, for example, misestimated emissions inventories.

## Visibility

Two separate modeling approaches were used to estimate changes in visibility degradation in the eastern and southwestern U.S. These are the two regions of the coterminous U.S. for which Clean Air Act programs were expected to have yielded the most significant reductions in visibility degradation. Visibility changes in the eastern 31 states were estimated based on the RADM/EM results for sulfates; and changes in visibility in 30 southwestern U.S. urban areas were calculated using a linear emissions scaling approach. Despite the potential significance of Clean Air Act-related visibility changes in southwestern U.S. Class I areas, such as National Parks, resource limitations precluded implementation of the analysis planned for these areas.

The RADM/EM system includes a post-processor which computes various measures of visibility degradation associated with changes in sulfate aerosols.[23] The basic approach is to allocate the light extinction budget for the eastern U.S. among various aerosols, including particulate sulfates, nitrates, and organics. The change in light extinction from sulfates is provided directly by RADM, thereby reflecting the complex formation and transport mechanisms associated with this most significant contributor to light extinction in the eastern U.S. Nitrates are not estimated directly by RADM. Instead, RADM-estimated concentrations of nitric acid are used as a surrogate to provide the basis for estimating changes in the particulate nitrate contribution to light extinction. The organic fractions were held constant between the two scenarios. Standard outputs include daylight distribution of light extinction, visual range, and DeciViews[24] for each of RADM's 80-km grid cells. For the present study, the RADM visibility post-processor was configured to provide the 90th percentile for light extinction and the 10th percentile for visual range to represent worst cases; and the 50th percentile for both of these to represent average cases. More detailed documentation of the RADM/EM system and the assumptions used to configure the visibility calculations are presented in the RADM Report (1995).

To estimate differences in control and no-control scenario visibility in southwestern U.S. urban areas, a modified linear rollback approach was developed and applied to 30 major urban areas with population greater than 100,000.[25] For each of the 30 urban centers, seasonal average 1990 air quality data was compiled for key pollutants, including $NO_2$ and $PM_{10}$, contributing to visibility degradation in southwestern U.S. coastal and inland cities. $PM_{10}$ was then speciated into its key components using city-specific annual average $PM_{10}$ profile data. After adjusting for regional — and for some species, city-specific— background levels, concentrations of individual light-attenuating species were scaled linearly based on changes in emissions of that pollutant or a proxy pollutant.[26] Using the same approach used for the 1993 EPA Report to Congress on effects of the 1990 Clean Air Act Amendments on visibility in Class I areas, light extinction coefficients for each of these species were then multiplied by their respective concentrations to derive a city-specific light extinction budget.[27] This process was repeated for pre-1990 control and all no-control scenarios by scaling 1990 results by the relative change in annual county-level emissions of $SO_x$, $NO_x$, and PM. Based on the city-specific light extinction budget calculations, measures for total extinction, visual range, and DeciView were calculated for each scenario and target year.

### Control scenario visibility

Unlike the other air quality conditions addressed in the present study, modeled visibility conditions are used as the basis for the control scenario rather than actual historical conditions. However, like the other air quality benefits of the historical Clean Air Act, it is the differences between modeled visibility outcomes for the control and no-control scenarios which are used

[23] A complete discussion, including appropriate references to other documents, of the RADM and RADM/EM modeling conducted for the present study is presented in the subsection on acid deposition earlier in this appendix.

[24] The DeciView Haze Index (dV) is a relatively new visibility indicator aimed at measuring visibility changes in terms of human perception. It is described in detail in the SAI SW Visibility Report (1994), pp. 4-2 to 4-3. See also Pitchford and Malm (1994) for the complete derivation of the DeciView index.

[25] Complete documentation of the linear scaling modeling, speciation methodologies, spatial allocation of emissions, and other data and assumptions are provided by the SAI SW Visibility Report (1994).

[26] For example, sulfate ($SO_4$) concentrations were scaled based on changes in sulfur oxide ($SO_x$) emissions.

[27] The term "light extinction budget" refers to the apportionment of total light attenuation in an area to the relevant pollutant species.

to estimate visibility benefits. Nevertheless, 1990 absolute levels of eastern U.S. visibility predicted by RADM under the control scenario are presented in Figure C-16 to provide a sense of initial visibility conditions.

For the southwestern urban areas, 1990 control scenario annual average light extinction budget, visual range, and DeciView conditions are listed in Table C-15. These 1990 results are presented to give the reader a sense of the initial visibility conditions in absolute, albeit approximate, terms.

Figure C-16. RADM-Predicted Visibility Degradation, Expressed in Annual Average DeciView, for Poor Visibility Conditions (90th Percentile Under the Control Scenario.

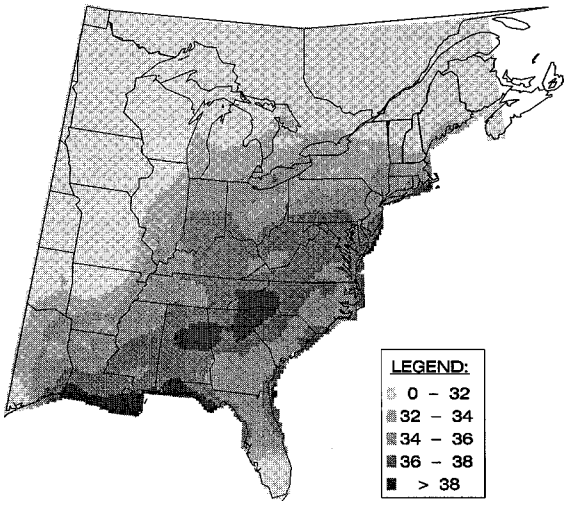


## *No-control scenario visibility*

The no-control scenario visibility results for the eastern U.S. area covered by RADM are presented in Figure C-17. No-control scenario 1990 outcomes for the 30 southwestern U.S. urban areas are presented in Table C-16.

Figure C-17. RADM-Predicted Visibility Degradation, Expressed in Annual Average DeciView, for Poor Visibility Conditions (90th Percentile Under the No-control Scenario.

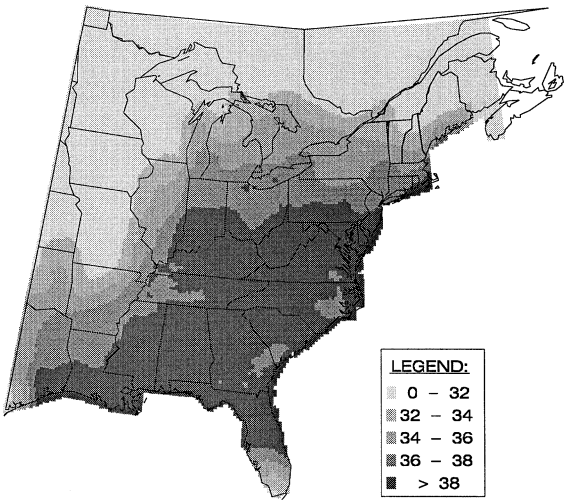


## *Summary differences in visibility*

### DeciView Haze Index

The DeciView Haze Index (dV) has recently been proposed as an indicator of the clarity of the atmosphere that is more closely related to human perception than visual range (VR) or total extinction ($b_{ext}$) (Pitchford and Malm, 1994). It is defined by the equation:

$$dV = 10\ 1ne\ (\frac{b_{ext}}{10}) \qquad (2)$$

where:

$b_{ext}$ = total extinction in inverse megameters ($Mm^{-1}$)

This index has the value of approximately 0 when the extinction coefficient is equal to the scattering coefficient for particle-free air (Rayleigh scattering) and increases in value by approximately one unit for each 10 percent increase in $b_{ext}$. Since the apparent change in visibility is related to the percent change in $b_{ext}$ (Pitchford et al., 1990), equal changes in dV correspond to approximately equally perceptible changes in visibility. Recent research indicates that, for most observers, a "just noticeable change" in visibility corresponds to an increase or decrease of about one to two dV units.

Table C-15. 1990 Control Scenario Visibility Conditions for 30 Southwestern U.S. Cities.

| City | Light Extinction Budget (b, $Mm^{-1}$) | Visual Range (km) | Deci View (dV) |
|---|---|---|---|
| Los Angeles, CA | 197.6 | 15.2 | 29.8 |
| San Bernardino, CA | 201.7 | 14.9 | 30.0 |
| Riverside, CA | 208.3 | 14.4 | 30.4 |
| Anaheim, CA | 170.1 | 17.6 | 28.3 |
| Ventura, CA | 113.3 | 26.5 | 24.3 |
| San Diego, CA | 126.9 | 23.6 | 25.4 |
| Santa Barbara, CA | 112.8 | 26.6 | 24.2 |
| Bakersfield, CA | 215.1 | 13.9 | 30.7 |
| Fresno, CA | 211.7 | 14.2 | 30.5 |
| Modesto, CA | 148.8 | 20.2 | 27.0 |
| Stockton, CA | 153.1 | 19.6 | 27.3 |
| San Francisco, CA | 120.8 | 24.8 | 24.9 |
| Oakland, CA | 117.5 | 25.5 | 24.6 |
| San Jose, CA | 154.6 | 19.4 | 27.4 |
| Monterey, CA | 84.7 | 35.4 | 21.4 |
| Sacramento, CA | 119.1 | 25.2 | 24.8 |
| Redding, CA | 83.2 | 36.1 | 21.2 |
| Reno, NV | 147.4 | 20.3 | 26.9 |
| Las Vegas, NV | 157.9 | 19.0 | 27.6 |
| Salt Lake City, UT | 117.5 | 25.5 | 24.6 |
| Provo, UT | 107.8 | 27.8 | 23.8 |
| Fort Collins, CO | 80.7 | 37.2 | 20.9 |
| Greeley, CO | 84.2 | 35.6 | 21.3 |
| **Denver, CO** | 153.4 | 19.6 | 27.3 |
| **Colorado Springs, CO** | 83.3 | 36.0 | 21.2 |
| Pueblo, CO | 88.1 | 34.1 | 21.8 |
| Albuquerque, NM | 91.1 | 32.9 | 22.1 |
| El Paso, TX | 109.3 | 27.5 | 23.9 |
| Tucson, AZ | 85.6 | 35.0 | 21.5 |
| **Phoenix, AZ** | **125.3** | **23.9** | **25.3** |

Data Source: SAI SW Visibility Report (1994).

Table C-16. 1990 No-control Scenario Visibility Conditions for 30 Southwestern U.S. Cities.

| City | Light Extinction Budget (b, $Mm^{-1}$) | Visual Range (km) | DeciView (dV) |
|---|---|---|---|
| Los Angeles, CA | 333.4 | 9.0 | 35.1 |
| San Bernardino, CA | 337.3 | 8.9 | 35.2 |
| Riverside, CA | 343.2 | 8.7 | 35.4 |
| Anaheim, CA | 286.3 | 10.5 | 33.5 |
| Ventura, CA | 194.8 | 15.4 | 29.7 |
| San Diego, CA | 210.1 | 14.3 | 30.4 |
| Santa Barbara, CA | 183.2 | 16.4 | 29.1 |
| Bakersfield, CA | 356.4 | 8.4 | 35.7 |
| Fresno, CA | 349.0 | 8.6 | 35.5 |
| Modesto, CA | 240.1 | 12.5 | 31.8 |
| Stockton, CA | 248.1 | 12.1 | 32.1 |
| San Francisco, CA | 197.3 | 15.2 | 29.8 |
| Oakland, CA | 188.6 | 15.9 | 29.4 |
| San Jose, CA | 253.0 | 11.9 | 32.3 |
| Monterey, CA | 141.4 | 21.2 | 26.5 |
| Sacramento, CA | 189.2 | 15.9 | 29.4 |
| Redding, CA | 128.6 | 23.3 | 25.5 |
| Reno, NV | 416.6 | 7.2 | 37.3 |
| Las Vegas, NV | 643.8 | 4.7 | 41.6 |
| Salt Lake City, UT | 185.8 | 16.1 | 29.2 |
| Provo, UT | 159.0 | 18.9 | 27.7 |
| Fort Collins, CO | 191.2 | 15.7 | 29.5 |
| Greeley, CO | 117.0 | 25.6 | 24.6 |
| Denver, CO | 284.4 | 10.5 | 33.5 |
| Colorado Springs, CO | 175.8 | 17.1 | 28.7 |
| Pueblo, CO | 299.9 | 10.0 | 34.0 |
| Albuquerque, NM | 175.8 | 17.1 | 28.7 |
| El Paso, TX | 276.3 | 10.9 | 33.2 |
| Tucson, AZ | 272.2 | 11.0 | 33.0 |
| **Phoenix, AZ** | **429.5** | **7.0** | **37.6** |

Data Source: SAI SW Visibility Report (1994).

Both VR and dV are measures of the value of $b_{ext}$ at one location in the atmosphere. Both are unaffected by the actual variability of the compositions and illumination of the atmosphere, so neither is closely linked to the human perception of a particular scene. The isolation of these parameters from site-specific variations and temporal fluctuations of the atmospheric illumination increases their usefulness for comparing the effects of air quality on visibility across a range of geographic locations for a range of time periods. Each parameter attempts to scale the $b_{ext}$ data so that changes in air quality can be used to provide an indication of changes in the human perception of a scene.

**Modeling Results**

The differences in modeled 1990 control and no-control scenario visibility conditions projected by the RADM/EM for the eastern U.S. are presented in Figure C-18. The map shows the percent increase in modeled annual average visibility degradation under poor conditions for 1990 when moving from the control to the no-control scenario. The results indicate perceptible differences in visibility between the control and no-control scenario throughout the RADM domain. The relatively large increase in visibility impairment in the Gulf Coast area is a reflection of the significant increases in 1990 sulfate concentrations associated with the no-control scenario. (See the earlier discussion of effects in this region in the sections dealing with acid deposition.)

Figure C-18. RADM-Predicted Increase in Visibility Degradation, Expressed in Annual Average DeciView, for Poor Visibility Conditions (90th Percentile) Under the No-control Scenario.

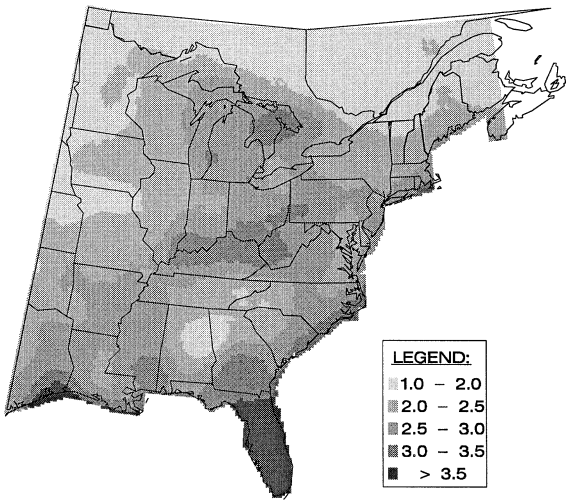


The differences in modeled 1990 control and no-control scenario visibility conditions in the 30 southwestern U.S. urban areas projected by linear rollback modeling are presented in Table C-17. When reviewing these visibility degradation differentials for the 30 southwestern U.S. urban areas, it is important to consider that while estimated differences in visual range were in many cases very large, changes in the DeciView Haze Index (dV) may be relatively small. This is because the perception of visibility degradation measured by dV may be small when baseline visibility is high.[28] Even so, the results indicate that, by 1990, visibility in southwestern U.S. urban areas would be noticeably worse under the no-control scenario.

## *Key caveats and uncertainties for visibility*

There are several sources of uncertainty in the RADM and southwestern U.S. linear scaling model analyses. For RADM, the use of nitric acid as a surrogate for estimating changes in light-attenuating nitrate particles ignores the interaction effects of nitrates, sulfates, and ammonia. As a result, increases in nitrates may be overestimated by the model when both sulfates and nitric acid increase. However, the significance of this potential overestimation is mitigated to some extent by the relative insignificance of nitrate-related visibility degradation relative to sulfates which prevails in the eastern U.S.

Several important uncertainties in the southwestern U.S. urban area visibility analysis are described in detail in the SAI SW Visibility Report (1994). First, the need to use seasonal average conditions leads to underestimation of extreme visibility impairment episodes associated with high humidity, since particle growth due to water absorption is highly nonlinear. Second, although the use of city-specific light extinction and PM speciation data is significantly better than reliance on regional averages, uncertainties in city-specific data may contribute to overall uncertainty in the estimates. However, overall uncertainty associated with these factors will be reduced to some extent since overestimation of visibility degradation in some cities

[28] See SAI SW Visibility Report (1994), page 5-3.

will be offset by underestimations in other cities. Finally, the linear scaling used to estimate the pre-1990 control scenarios and the no-control scenarios was based on changes in county-wide or air basin emissions. Uncertainties associated with apportionment of state-wide emission changes to individual counties or air basins may contribute significantly to overall uncertainty in the visibility change estimates. Such apportionment is particularly difficult for $SO_x$ emission changes, since emission reductions achieved by the Clean Air Act tended to be at relatively remote utility and smelter plants. However, sulfates are a relatively minor source of light attenuation in western urban areas.

An important overall limitation of the visibility analysis conducted for the present study is that only southwestern urban areas and the eastern 31 states were included. The Clean Air Act may have contributed toward significant reductions in visibility degradation in other areas. For example, Clean Air Act programs to reduce ambient particulate matter may have motivated reductions in silvicultural burning in some northwestern states. Perhaps the greatest deficiency in geographic coverage by the present study is the omission of visibility changes in Class I areas in the west.

Table C-17. Summary of Relative Change in Visual Range and DeciView Between 1990 Control and No-control Scenario Visibility Conditions for 30 Southwestern U.S. Cities.

| City | Visual Range (%) | DeciView (dV) |
|---|---|---|
| Los Angeles, CA | 69 | -5 |
| San Bernardino, CA | 67 | -5 |
| Riverside, CA | 65 | -5 |
| Anaheim, CA | 68 | -5 |
| Ventura, CA | 72 | -5 |
| San Diego, CA | 65 | -5 |
| Santa Barbara, CA | 62 | -5 |
| Bakersfield, CA | 66 | -5 |
| Fresno, CA | 65 | -5 |
| Modesto, CA | 61 | -5 |
| Stockton, CA | 62 | -5 |
| San Francisco, CA | 63 | -5 |
| Oakland, CA | 61 | -5 |
| San Jose, CA | 64 | -5 |
| Monterey, CA | 67 | -5 |
| Sacramento, CA | 59 | -5 |
| Redding, CA | 55 | -4 |
| Reno, NV | 183 | -10 |
| Las Vegas, NV | 308 | -14 |
| Salt Lake City, UT | 58 | -5 |
| Provo, UT | 48 | -4 |
| Fort Collins, CO | 137 | -9 |
| Greeley, CO | 39 | -3 |
| Denver, CO | 85 | -6 |
| Colorado Springs, CO | 111 | -7 |
| Pueblo, CO | 240 | -12 |
| Albuquerque, NM | 93 | -7 |
| El Paso, TX | 153 | -9 |
| Tucson, AZ | 218 | -12 |
| Phoenix, AZ | 243 | -12 |

Data Source: SAI SW Visibility Report (1994).

## Air Quality Modeling References


Chang. 1995. *SARMAP Air Quality Model (SAQM).* Final report to San Joaquin Valley wide Air Pollution Study Agency.

DaMassa, Tanrikulu, and Ranzier. 1996. *Photochemical Modeling of August 3-6, 1990, Ozone Episode in Central California Using the SARMAP Air Quality Model. Part II: Sensitivity and Diagnostic Testing.* Preprints, Ninth Joint Conference on the Applications of Air Pollution Meteorology with Air Waste Management Association. January 28 - February 2, 1996, Atlanta, Georgia.

Dennis, R. 1995. *Estimation of Regional Air Quality and Deposition Changes Under Alternative 812 Emissions Scenarios Predicted by the Regional Acid Deposition Model, RADM*. Draft Report for U.S. Environmental Protection Agency, ORD/NERL. October 1995.

ICF Kaiser/Science Applications International. 1996. *PM Interpolation Methodology for the Section 812 Retrospective Analysis*. Memorandum from J. Langstaff to Jim DeMocker.

ICF Kaiser/Systems Applications International. 1994. *Retrospective Analysis of the Impact of the Clean Air Act on Urban Visibility in the Southwestern United States.* Final Report.

ICF Kaiser/Systems Applications International. 1995. *Retrospective Analysis of Ozone Air Quality in the United States*. Final Report.

ICF Kaiser/Systems Applications International. 1992. *Retrospective Analysis of Particulate Matter Air Quality in the United States*. Draft Report.

ICF Kaiser/Systems Applications International. 1995. *Retrospective Analysis of Particulate Matter Air Quality in the United States*. Final Report.

ICF Kaiser/Systems Applications International. 1994. *Retrospective Analysis of $SO_x$, $NO_x$ and CO Air Quality in the United States*. Final Report.

ICF Resources Incorporated. 1992. *Results of Retrospective Electric Utility Clean Air Act Analysis - 1980, 1985, and 1990.* September 30.

Pitchford, Marc L. and William C. Malm. 1994. "Development and Applications of a Standard Visual Index." *Atmospheric Environment*, vol. 28, no. 5. pp. 1049-1054.

Seaman and Stauffer. 1995. *Development and Design Testing of the SARMAP Meteorological Model.* Final report to San Joaquin Valley wide Air Pollution Study Agency.

Seaman, Stauffer, and Lario-Gibbs. 1995. "A Multi-Scale Four Dimensional Data Assimilation System Applied in the San Joaquin Valley During SARMAP. Part I: Modeling Design and Basic Performance Characteristics." *Journal of Applied Meteorology*. Volume 34. In press.

Tanrikulu, DaMassa, and Ranzieri. 1996. *Photochemical Modeling of August 3-6, 1990 Ozone Episode in Central California Using the SARMAP Air Quality Model. Part I: Model Formulation, Description and Basic Performance.* Preprints. Ninth Joint Conference on the Application of Air Pollution Meteorology with Air Waste Management Association. January 28 - February 2, 1996. Atlanta, Georgia.

Trijonis. 1990. *Visibility: Existing and Historical Conditions--Causes and Effects*. NAPAP Report 24. 1990.

U.S. Environmental Protection Agency (EPA). 1989. *Procedures for Applying City-Specific EKMA.* EPA-450/4-89-012. Office of Air Quality Planning and Standards.